Comparison between different viewpoints on bulk growth mechanics

NISSUNA UMANA INVESTIGAZIONE SI PUO DIMANDARE VERA SCIENZIA
S'ESSA NON PASSA PER LE MATEMATICHE DIMOSTRAZIONI
LEONARDO DA VINCI

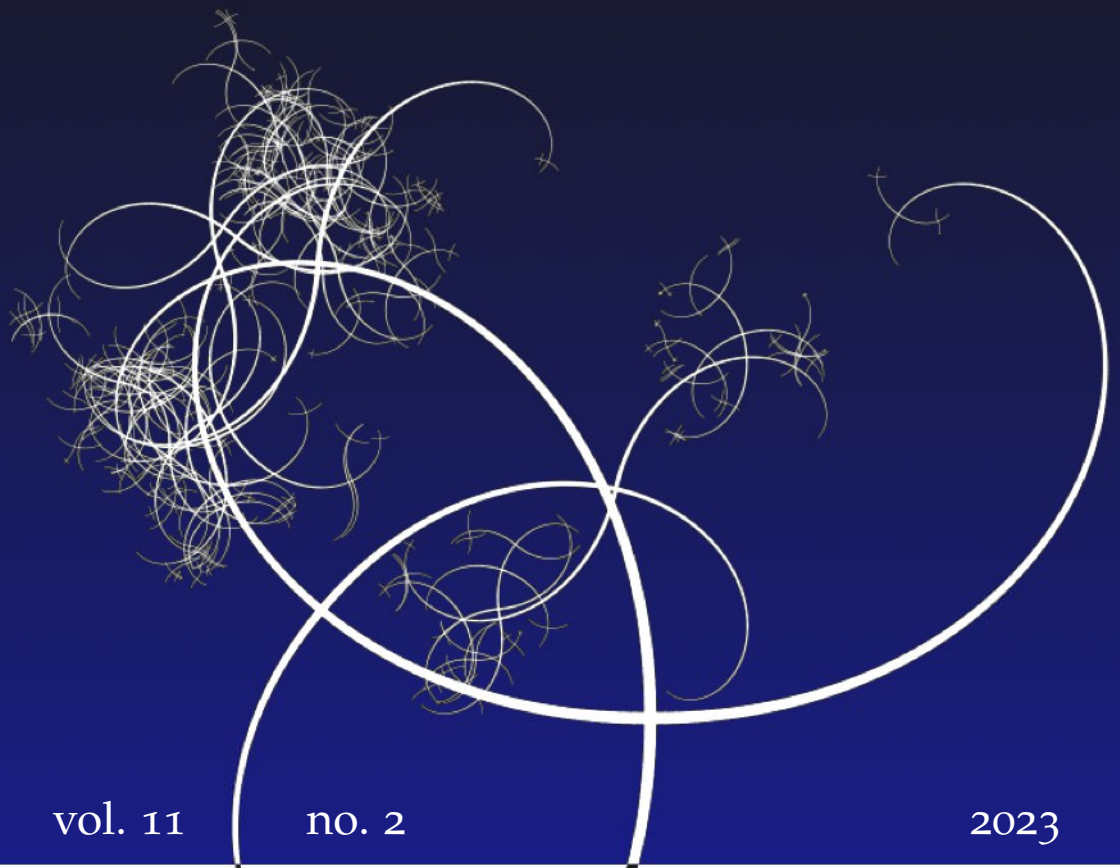

vol. 11 no. 2 2023

Mathematics and Mechanics *of* Complex Systems

Alfio Grillo and Salvatore Di Stefano

COMPARISON BETWEEN DIFFERENT VIEWPOINTS ON BULK GROWTH MECHANICS

msp

MATHEMATICS AND MECHANICS OF COMPLEX SYSTEMS
Vol. 11 (2023), No. 2, pp. 287–311
DOI: 10.2140/memocs.2023.11.287

COMPARISON BETWEEN DIFFERENT VIEWPOINTS ON BULK GROWTH MECHANICS

ALFIO GRILLO AND SALVATORE DI STEFANO

This work brings together two viewpoints on the mechanics of bulk growth that, in spite of some similarities, originate from different conceptualizations of this phenomenon. Each viewpoint designates a specific approach to growth, identified by the "growth law" that it determines, i.e., the "rule" governing the mass variation in the considered growing medium. In the first approach, which we call the "a priori approach", the growth law is supplied phenomenologically, is viewed as a constraint, and is appended to the principle of virtual work in order to determine the effective dynamic equations of the growth problem at hand. On the other hand, in the second approach, denominated the "a posteriori approach", growth is regarded as an unconstrained problem, and the growth law is viewed as a consequence of the medium's dynamics. To highlight the main differences between these two approaches, we solve numerically a simple benchmark problem, and we compare the simulations obtained for each approach.

1. Introduction

Within a research line begun with [Grillo et al. 2019a; 2019b], and continued in [Licari 2021; Grillo and Di Stefano 2023a; 2023b], we consider two different approaches to the volumetric growth of tumor tissues and we analyze them by modifying and solving numerically a benchmark test available in the literature. In particular, following [Grillo and Di Stefano 2023a; 2023b; 2023c], we distinguish the case in which a growth law is given "a priori", that is, on the *"basis of phenomenological observation"* [Ambrosi and Preziosi 2002], from the case in which it is obtained "a posteriori", that is, as a manifestation of the evolution of the kinematic parameter that describes the variation of mass of the tissue under study and the structural transformations associated with it (see also sections 1.1. and 4.1. of [Grillo et al. 2019b], although it addresses the approach termed here "a priori"). Contextually, we refer to these viewpoints as the "a priori" and the "a posteriori" approach, respectively [Grillo and Di Stefano 2023a].

Communicated by Francesco dell'Isola.
MSC2020: 65Z05, 74B20, 74F25, 92B05, 92F99.
Keywords: growth phenomenology, principle of virtual work, benchmark tests.

As shown by [Grillo and Di Stefano 2023b; 2023c], within the "a priori" approach, the growth law is regarded as a *"nonholonomic and rheonomic constraint"* (see also [Grillo et al. 2019b]), which has to be appended to the principle of virtual work, for example, according to the formulation of [DiCarlo and Quiligotti 2002]. As an extension of such an approach, Grillo and Di Stefano [2023b; 2023c] also consider a generalization of the work [Gurtin 1996] on the use of the Cahn–Hilliard model for systems with variable mass. In this case, growth is described by a single kinematic descriptor, which acquires the role of order parameter of the theory, and a model of growth of grade one in this parameter is designed. The main feature of the a priori approach is that the growth law is a function of the mass fraction of chemical substances, called *nutrients*, which regulate the accretion or the resorption of mass.

Following a different perspective, the "a posteriori" approach, whose rationale was indicated by [Grillo et al. 2019a], in an elaboration of the framework of [Ambrosi and Guana 2007; Ambrosi and Guillou 2007], does not prescribe any growth law, nor does it place restrictions on the kinematic descriptor associated with growth, apart from those that may stem, for example, from possible geometric symmetries of the considered problem. Therefore, the growth law is determined as a consequence of the dynamics [Ambrosi and Guana 2007; Grillo and Di Stefano 2023a; Licari 2021]. This idea, which, to our knowledge, was first put forward by [Epstein and Maugin 2000] within a description of growth completely different from the one addressed here, has been recently refined in [Grillo and Di Stefano 2023a], where the theory behind the "a posteriori" approach is formalized and contextualized to the biologically relevant case of tumor growth (an explorative numerical simulation of this problem in a simplified setting, based essentially on the viewpoints presented by [Grillo et al. 2019a; 2019b], has been done by [Licari 2021]). In this respect, it is important to recall that this approach is intended to be a *"step forward"* [Grillo and Di Stefano 2023a] in the direction of the theory of growth proposed by [DiCarlo and Quiligotti 2002] and, thus, it is not new per se. Rather, it is the interpretation of some of its implications that is new, especially if contextualized to a specific selection of the constitutive framework and, more importantly, of the growth-conjugated external generalized forces.

We reconcile these two approaches by considering a mixed situation in which it is required that the growth law for mass accretion be identically zero in the absence of a sufficient amount of nutrients, whereas no a priori conditions are put on it when nutrients are available with sufficient concentration, and a specular definition of the mass variation is hypothesized for mass resorption. In other words, we let the availability of nutrients activate or deactivate the variation of mass of the body, but, once such variation occurs, we let it be driven by the balance of all the generalized forces expending power, or work, on the velocity associated with the growth parameter.

As a proof of concept, we solve the initial and boundary value problems (IBVPs)

formulated in the sequel of this work by adhering to the computational framework developed by [Di Stefano et al. 2018; Grillo et al. 2019b; Ramírez-Torres et al. 2021], and adopted by [Licari 2021], which reformulates and generalizes the study originally designed by [Ambrosi and Mollica 2002], and which we further extend to account for our setting. For our purposes, we consider *"the growth of a ductal carcinoma [...] inside a breast duct"* [Ambrosi and Mollica 2002], which is modeled as a cylinder with underformable lateral wall. This way, when the advancement of the tumor takes place, it is forced to proceed along the cylinder's axial direction only [Ambrosi and Mollica 2002]. The numerical results are discussed and compared with the predictions presented by [Grillo and Di Stefano 2023a; 2023b], with those of [Di Stefano et al. 2018; Grillo et al. 2019b], and with some of the preliminary outcomes obtained by [Licari 2021].

2. Evolution of the nutrient substances

For future use, we invoke the Bilby–Kröner–Lee decomposition of the deformation gradient tensor, that is, $\boldsymbol{F} = \boldsymbol{F}_{\mathrm{e}}\boldsymbol{K}$, where $\boldsymbol{F}_{\mathrm{e}}$ and $\boldsymbol{K}$ are said to be the tensor of elastic distortions and the growth tensor, respectively. We introduce the determinant $J_{\boldsymbol{K}} = \det \boldsymbol{K}$, which satisfies the identity $\dot{J}_{\boldsymbol{K}} = J_{\boldsymbol{K}} \operatorname{tr}(\boldsymbol{K}^{-1}\dot{\boldsymbol{K}})$.

For all three considered approaches, i.e., the a priori, the a posteriori, and the mixed approach, and within the adopted monophasic framework [Grillo and Di Stefano 2023a], nutrients are assumed to evolve according to a diffusion-reaction equation that, granted Fick's law, and in material formalism, reads [Ambrosi and Preziosi 2002; Ambrosi and Guillou 2007; Grillo et al. 2012; Di Stefano et al. 2018; Mascheroni et al. 2018; Ramírez-Torres et al. 2021; Andreucci et al. 2022]

$$\partial_t(\varrho_{\mathrm{R}}\omega) - \operatorname{Div}(\varrho_{\mathrm{R}}\boldsymbol{D}\operatorname{Grad}\omega) = -\varrho_{\mathrm{R}} r_{\mathrm{n}}\omega, \tag{1}$$

where ϱ_{R} is the mass density of the medium per unit volume of the reference placement $\mathscr{B}$, ω is the mass fraction of the nutrients, r_{n} is the rate at which the nutrients are absorbed, and $\boldsymbol{D}$ is the material diffusivity tensor. By expanding the term $\partial_t(\varrho_{\mathrm{R}}\omega)$, and using the identity $\varrho_{\mathrm{R}} = J_{\boldsymbol{K}}\varrho_\nu$, with ϱ_ν being the mass density of the medium in the natural state, assumed to be constant, (1) becomes

$$J_{\boldsymbol{K}}\varrho_\nu\dot{\omega} - \operatorname{Div}(J_{\boldsymbol{K}}\varrho_\nu\boldsymbol{D}\operatorname{Grad}\omega) = -J_{\boldsymbol{K}}\varrho_\nu r_{\mathrm{n}}\omega - J_{\boldsymbol{K}}\varrho_\nu\omega\operatorname{tr}(\boldsymbol{K}^{-1}\dot{\boldsymbol{K}}). \tag{2}$$

In the case of isotropic medium, the material diffusivity tensor $\boldsymbol{D}$ can be taken as

$$\boldsymbol{D} := d_0\boldsymbol{C}^{-1} + d_1\boldsymbol{K}^{-1}.\boldsymbol{K}^{-\mathrm{T}} + d_2[\boldsymbol{K}^{-1}.\boldsymbol{K}^{-\mathrm{T}}]\boldsymbol{C}[\boldsymbol{K}^{-1}.\boldsymbol{K}^{-\mathrm{T}}], \tag{3}$$

where d_0, d_1, and d_2 are scalar-valued functions defined by $d_n := d_{n\mathrm{R}}J_{\boldsymbol{K}}^{2n}/J^{2n}$, for $n = 0, 1, 2$, $d_{n\mathrm{R}}$ is a referential diffusivity [Ateshian and Weiss 2010], and $\boldsymbol{C}$ is the right Cauchy–Green deformation tensor, defined, with a slight abuse of notation,

as $\boldsymbol{C} = \boldsymbol{F}^{\mathrm{T}}.\boldsymbol{F}$ (in the sequel, for simplicity, we set $d_{n\mathrm{R}} = d_{0\mathrm{R}}$ for $n = 0, 1, 2$). A more precise definition of $\boldsymbol{C}$, based on the works [Federico 2012; Federico et al. 2016], has been presented by [Grillo and Di Stefano 2023b], where the kinematics of a growing body is discussed in deeper detail. We finally recall that the definition reported in (3) is similar to the one introduced by [Ateshian and Weiss 2010] for characterizing the material permeability of isotropic media. In a recent work, (3) has been adapted to formulate a possible constitutive representation of the permeability tensor within a study of the remodeling of multicellular spheroids subjected to compression-release tests [Di Stefano et al. 2022].

With respect to the time window $[t_{\mathrm{in}}, t_{\mathrm{fin}}]$, the evolution of the nutrients will be described by the solution of the initial and boundary value problem

$$
\begin{aligned}
&J_{\boldsymbol{K}}\varrho_{\nu}\dot{\omega} \\
&= \mathrm{Div}(J_{\boldsymbol{K}}\varrho_{\nu}\boldsymbol{D}\,\mathrm{Grad}\,\omega) - J_{\boldsymbol{K}}\varrho_{\nu}r_{\mathrm{n}}\omega - J_{\boldsymbol{K}}\varrho_{\nu}\omega\,\mathrm{tr}(\boldsymbol{K}^{-1}\dot{\boldsymbol{K}}), && \mathscr{B}\times\,]t_{\mathrm{in}}, t_{\mathrm{fin}}], && \text{(4a)}\\
&\omega = \omega_{\mathrm{b}}, && \partial^{\omega}_{\mathrm{D}}\mathscr{B}\times\,]t_{\mathrm{in}}, t_{\mathrm{fin}}], && \text{(4b)}\\
&[-J_{\boldsymbol{K}}\varrho_{\nu}\boldsymbol{D}\,\mathrm{Grad}\,\omega]\boldsymbol{N} = \jmath_{\mathrm{b}}, && \partial^{\omega}_{\mathrm{N}}\mathscr{B}\times\,]t_{\mathrm{in}}, t_{\mathrm{fin}}], && \text{(4c)}\\
&\omega(X, t_{\mathrm{in}}) = \omega_{\mathrm{in}}(X), && \mathscr{B}, && \text{(4d)}
\end{aligned}
$$

where ω_{b} is a mass fraction prescribed on the Dirichlet boundary $\partial^{\omega}_{\mathrm{D}}\mathscr{B}$ associated with the nutrients, $\jmath_{\mathrm{b}}$ is a mass flux imposed on the Neumann boundary $\partial^{\omega}_{\mathrm{N}}\mathscr{B}$, and $\omega_{\mathrm{in}}(X)$ is the initial distribution of the nutrients.

Note that, if the balance of mass holds true in the form $\dot{\varrho}_{\mathrm{R}} = Jr_{\gamma} = J_{\boldsymbol{K}}\varrho_{\nu}R_{\gamma}$ (see [Epstein and Maugin 2000; Lubarda and Hoger 2002; Ambrosi and Preziosi 2002; Grillo and Di Stefano 2023a; 2023b]), which yields $\mathrm{tr}(\boldsymbol{K}^{-1}\dot{\boldsymbol{K}}) = R_{\gamma}$, and if R_{γ} is known from the outset, as is the case in the "a priori" approach, then R_{γ} can be used in lieu of $\mathrm{tr}(\boldsymbol{K}^{-1}\dot{\boldsymbol{K}})$ in (2) and (4a).

3. The "a priori" vs. the "a posteriori" approach to growth

From here on, we refer to the "a priori approach" and to the "a posteriori approach" with the abbreviated notation "approach A1" and "approach A2", respectively.

3.1. ***The approach A1.*** Based on the framework developed by [Grillo and Di Stefano 2023b], we consider the mass balance law in the form of a *"nonholonomic and rheonomic constraint on the growth tensor"* $\boldsymbol{K}$. Hence, we set (see equation (7) of [Grillo and Di Stefano 2023b])

$$
\hat{\mathcal{C}}_{\boldsymbol{K}} \circ (\boldsymbol{F}, \boldsymbol{K}, \dot{\boldsymbol{K}}, \omega) := \boldsymbol{K}^{-\mathrm{T}} : \dot{\boldsymbol{K}} - [\hat{R}_{\gamma(\mathrm{ph})} \circ (\boldsymbol{F}, \boldsymbol{K}, \omega)] = 0, \tag{5}
$$

thereby defining phenomenologically the rate of mass accretion or resorption as $R_{\gamma} := R_{\gamma(\mathrm{ph})} \equiv \hat{R}_{\gamma(\mathrm{ph})} \circ (\boldsymbol{F}, \boldsymbol{K}, \omega)$. In particular, following [Mascheroni et al. 2016; 2018], and adopting the notation of [Grillo and Di Stefano 2023a; 2023b], we

consider the growth law (adapted from [Ambrosi and Preziosi 2002; Byrne and Preziosi 2003])

$$\hat{R}_{\gamma(\mathrm{ph})} \circ (\boldsymbol{F}, \boldsymbol{K}, \omega) := \zeta_{\mathrm{a}} \langle h_{\mathrm{a}} \circ \omega \rangle_{+} \left[1 - \frac{\alpha \langle \hat{\wp} \circ (\boldsymbol{F}, \boldsymbol{K}) \rangle_{+}}{\sigma_{\mathrm{c}} + \langle \hat{\wp} \circ (\boldsymbol{F}, \boldsymbol{K}) \rangle_{+}} \right] - \zeta_{\mathrm{r}} \langle h_{\mathrm{r}} \circ \omega \rangle_{+}, \quad (6)$$

where the dependence of $\hat{R}_{\gamma(\mathrm{ph})}$ on $\boldsymbol{F}$ and $\boldsymbol{K}$ is inherited from the stress measure $\hat{\wp} \circ (\boldsymbol{F}, \boldsymbol{K})$, here taken equal to the hydrostatic Cauchy pressure, i.e., $\hat{\wp} \circ (\boldsymbol{F}, \boldsymbol{K}) := -\frac{1}{3} \operatorname{tr}[\hat{\boldsymbol{\sigma}} \circ (\boldsymbol{F}, \boldsymbol{K})]$; $\hat{\boldsymbol{\sigma}} \circ (\boldsymbol{F}, \boldsymbol{K})$ is the constitutive function of Cauchy stress; the operator $\langle \cdot \rangle_{+}$ and the functions h_{a} and h_{r} (see [Grillo and Di Stefano 2023a]) are defined by

$$h_{\mathrm{a}} \circ \omega = \frac{\omega - \omega_{\mathrm{cr}}}{\omega_{\mathrm{env}} - \omega_{\mathrm{cr}}}, \qquad h_{\mathrm{r}} \circ \omega = 1 - \frac{\omega}{\omega_{\mathrm{cr}}}, \qquad \langle f \rangle_{+} := \tfrac{1}{2}[f + |f|] \quad \text{for all } f. \quad (7)$$

Here, ω_{env} and ω_{cr} are constant parameters that represent the nutrients' mass fraction in the "bath" in which the medium is immersed and a threshold value of the nutrients' mass fraction in the medium below which the accretion of mass of the medium itself cannot take place. In particular, we assume $\omega_{\mathrm{env}} > \omega_{\mathrm{cr}}$. The other parameters featuring in (6) are the reciprocals of the time constants characterizing the accretion and resorption of mass, i.e., $\zeta_{\mathrm{a}} > 0$ and $\zeta_{\mathrm{r}} > 0$, and the positive constants α and σ_{c}, which ponderate the influence of mechanical stress on the overall growth law.

Within the approach A1 [Grillo and Di Stefano 2023b], and by neglecting body forces, the growth problem under study can be posed in the form of the initial and boundary value problem (IBVP)

$$\operatorname{Div} \boldsymbol{P} = \boldsymbol{0}, \qquad \mathscr{B} \times]t_{\mathrm{in}}, t_{\mathrm{fin}}], \quad (8a)$$

$$\chi = \chi_{\mathrm{b}}, \qquad \partial_{\mathrm{D}}^{\chi}\mathscr{B} \times]t_{\mathrm{in}}, t_{\mathrm{fin}}], \quad (8b)$$

$$\boldsymbol{P}\boldsymbol{N} = \boldsymbol{\tau}, \qquad \partial_{\mathrm{N}}^{\chi}\mathscr{B} \times]t_{\mathrm{in}}, t_{\mathrm{fin}}], \quad (8c)$$

$$J_{\boldsymbol{K}} \mathfrak{b}_{\nu} \operatorname{dev}\{\boldsymbol{C}\boldsymbol{K}^{-1}\dot{\boldsymbol{K}}\boldsymbol{C}^{-1} + \dot{\boldsymbol{K}}^{\mathrm{T}}\boldsymbol{K}^{-\mathrm{T}}\} = -\operatorname{dev}\boldsymbol{H} + \operatorname{dev}\boldsymbol{Z}, \qquad \mathscr{B} \times]t_{\mathrm{in}}, t_{\mathrm{fin}}], \quad (8d)$$

$$2J_{\boldsymbol{K}} \mathfrak{c}_{\nu} \operatorname{skew}[(\boldsymbol{K}^{-1}\dot{\boldsymbol{K}})\boldsymbol{C}^{-1}] = \boldsymbol{0}, \qquad \mathscr{B} \times]t_{\mathrm{in}}, t_{\mathrm{fin}}], \quad (8e)$$

$$\boldsymbol{K}^{-\mathrm{T}} : \dot{\boldsymbol{K}} = R_{\gamma(\mathrm{ph})}, \qquad \mathscr{B} \times]t_{\mathrm{in}}, t_{\mathrm{fin}}], \quad (8f)$$

$$\boldsymbol{K}(X, t_{\mathrm{in}}) = \boldsymbol{K}_{\mathrm{in}}(X), \qquad \mathscr{B}, \quad (8g)$$

where $\boldsymbol{P}$ is the first Piola–Kirchhoff stress tensor, χ is the motion, χ_{b} is the prescription of χ on the Dirichlet boundary $\partial_{\mathrm{D}}^{\chi}\mathscr{B}$, $\boldsymbol{\tau}$ is a contact force applied on the Neumann boundary $\partial_{\mathrm{N}}^{\chi}\mathscr{B}$, $\boldsymbol{N}$ is the field of conormals of $\partial\mathscr{B}$ (the superscript "χ" indicates that $\partial_{\mathrm{D}}^{\chi}\mathscr{B}$ and $\partial_{\mathrm{N}}^{\chi}\mathscr{B}$ are associated with the motion χ), $\mathfrak{b}_{\nu}$ and $\mathfrak{c}_{\nu}$ are material coefficients defining the constitutive expression of the dissipative part of the generalized internal force conjugated with growth (see [Grillo and Di Stefano 2023b]), $\boldsymbol{H}$ is the Eshelby stress tensor, $\boldsymbol{Z}$ is a generalized external force conjugated

with growth [DiCarlo and Quiligotti 2002], and $\boldsymbol{K}_{\text{in}}(X)$ is the initial distribution of the growth tensor. Note that the left-hand-sides of (8d) and (8e) are obtained by working out the dissipative part of the growth-conjugated, generalized internal force termed $\boldsymbol{Y}_{\text{u}}$ by [Grillo and Di Stefano 2023b], which reads

$$\boldsymbol{Y}_{\text{u,d}} = \tfrac{1}{3} J_{\boldsymbol{K}} \mathfrak{a}_\nu \operatorname{tr}(\boldsymbol{K}^{-1}\dot{\boldsymbol{K}})\boldsymbol{I}^{\text{T}} + 2J_{\boldsymbol{K}} \mathfrak{b}_\nu \boldsymbol{C} \operatorname{sym}[(\boldsymbol{K}^{-1}\dot{\boldsymbol{K}})\boldsymbol{C}^{-1}] + 2J_{\boldsymbol{K}} \mathfrak{c}_\nu \boldsymbol{C} \operatorname{skew}[(\boldsymbol{K}^{-1}\dot{\boldsymbol{K}})\boldsymbol{C}^{-1}]. \quad (9)$$

We remark that the operator "dev" in (8d), which extracts the deviatoric part of the tensor to which it is applied, acts on "mixed" second-order tensors, as is the case of $\boldsymbol{H}$ and $\boldsymbol{Z}$, i.e., on tensors of the type $\boldsymbol{A} = A_M{}^N \boldsymbol{E}^M \otimes \boldsymbol{E}_N$. In this circumstance, the operator "dev" is defined through the transpose of the identity tensor $\boldsymbol{I}$, so that $\operatorname{dev}\boldsymbol{A} := \boldsymbol{A} - \frac{1}{3}(\operatorname{tr}\boldsymbol{A})\boldsymbol{I}^{\text{T}} = \boldsymbol{A} - \frac{1}{3}(\boldsymbol{I} : \boldsymbol{A})\boldsymbol{I}^{\text{T}}$, with the identity $\operatorname{tr}\boldsymbol{A} = \boldsymbol{I} : \boldsymbol{A} = A_I{}^I$ holding true [Marsden and Hughes 1983]. Note that we shall use the same symbols "dev" and "tr" also for tensors of the type $\boldsymbol{T} = T^{AB}\boldsymbol{E}_A \otimes \boldsymbol{E}_B$, although, in such cases, $\operatorname{tr}\boldsymbol{T}$ is understood as $\operatorname{tr}\boldsymbol{T} = \boldsymbol{G} : \boldsymbol{T} = G_{AB}T^{AB}$, with G_{AB} being the components of the material metric tensor $\boldsymbol{G}$, and, accordingly, $\operatorname{dev}\boldsymbol{T} = \boldsymbol{T} - \frac{1}{3}(\operatorname{tr}\boldsymbol{T})\boldsymbol{G}^{-1} = \boldsymbol{T} - \frac{1}{3}(\boldsymbol{G} : \boldsymbol{T})\boldsymbol{G}^{-1}$. Finally, with the purpose of not introducing additional notation, the trace of the Cauchy stress tensor used in the definition of $\hat{\wp} \circ (\boldsymbol{F}, \boldsymbol{K})$ is understood here as $\operatorname{tr}[\hat{\boldsymbol{\sigma}} \circ (\boldsymbol{F}, \boldsymbol{K})] = \boldsymbol{g} : [\hat{\boldsymbol{\sigma}} \circ (\boldsymbol{F}, \boldsymbol{K})]$, where $\boldsymbol{g}$ is the spatial metric expressed as a function of material points and time, provided $\hat{\boldsymbol{\sigma}} \circ (\boldsymbol{F}, \boldsymbol{K})$ is assumed to have contravariant components.

To solve the system (8a)–(8g), one has to consider the evolution of the mass fraction of the nutrients through the solution of (4a)–(4d), with $R_{\gamma(\text{ph})}$ replacing $\operatorname{tr}(\boldsymbol{K}^{-1}\dot{\boldsymbol{K}})$.

To complete the picture, we also need to compute the Lagrange multiplier associated with the constraint (5), denoted by $\mu_{\boldsymbol{K}}$ (see [Grillo and Di Stefano 2023b; 2023c]), i.e.,

$$\mu_{\boldsymbol{K}} = \tfrac{1}{3}\operatorname{tr}\boldsymbol{Z} - \tfrac{1}{3}\operatorname{tr}\boldsymbol{H} - \tfrac{1}{3}J_{\boldsymbol{K}}[\mathfrak{a}_\nu + 2\mathfrak{b}_\nu]R_{\gamma(\text{ph})}, \qquad \mathscr{B} \times]t_{\text{in}}, t_{\text{fin}}]. \quad (10)$$

Finally, to handle the constraint (5), [Grillo and Di Stefano 2023b; 2023c] took a suggestion from [Nadile 1950] and treated time as a fictitious and constrained Lagrangian parameter, $\mathfrak{T}$ (see also the discussion on this topic reported in [Grillo and Di Stefano 2023c]). This, in turn, required an additional Lagrange multiplier $\mu_{\mathfrak{T}}$ and a fictitious generalized, scalar-valued force $\mathcal{Y}_{\text{u}} - \mathcal{Z}$, whose equations, holding in $\mathscr{B} \times]t_{\text{in}}, t_{\text{fin}}]$, are given by

$$\mu_{\mathfrak{T}} = -\mu_{\boldsymbol{K}} R_{\gamma(\text{ph})} = -\left\{\tfrac{1}{3}\operatorname{tr}\boldsymbol{Z} - \tfrac{1}{3}\operatorname{tr}\boldsymbol{H} - \tfrac{1}{3}J_{\boldsymbol{K}}[\mathfrak{a}_\nu + 2\mathfrak{b}_\nu]R_{\gamma(\text{ph})}\right\}R_{\gamma(\text{ph})}, \quad (11a)$$

$$\mathcal{Y}_{\text{u}} - \mathcal{Z} = -\mu_{\mathfrak{T}} = \mu_{\boldsymbol{K}} R_{\gamma(\text{ph})} = \left\{\tfrac{1}{3}\operatorname{tr}\boldsymbol{Z} - \tfrac{1}{3}\operatorname{tr}\boldsymbol{H} - \tfrac{1}{3}J_{\boldsymbol{K}}[\mathfrak{a}_\nu + 2\mathfrak{b}_\nu]R_{\gamma(\text{ph})}\right\}R_{\gamma(\text{ph})}. \quad (11b)$$

Remark 1 (the chemo-mechanical coupling in the approach A1). Since in the approach A1 the nutrients are considered, on physical grounds, in the definition

of the phenomenological growth law $R_{\gamma(\mathrm{ph})}$ and, consequently, in the equation determining the spherical part of the rate $\boldsymbol{K}^{-1}\dot{\boldsymbol{K}}$, i.e., (8f), their evolution must be studied *together* with the dynamics of χ and $\boldsymbol{K}$. Therefore, the system (8a)–(8g) has to be coupled with the initial and boundary value problem (4a)–(4d). Since this coupling manifests itself already through $R_{\gamma(\mathrm{ph})}$, it would remain also in the case in which the constitutive laws of $\boldsymbol{P}$ and $\boldsymbol{H}$ as well as the expressions of $\boldsymbol{Z}$ and of the coefficients $\mathfrak{a}_\nu$, $\mathfrak{b}_\nu$, and $\mathfrak{c}_\nu$ were taken to be independent of ω.

We finally notice that, recently, in theoretical mechanics there seems to be a renewed interest for continuum mechanical systems subjected to constraints and approached with the method of Lagrange multipliers, and some investigations on this subject have been summarized by [Bersani et al. 2020; dell'Isola and Di Cosmo 2018].

3.2. ***The approach A2.*** In the sequel, we do not repeat the whole rationale at the basis of the approach A2, since it has already been presented in [Grillo and Di Stefano 2023a], and we simply report the initial and boundary value problem which it leads to, i.e.,

$$\operatorname{Div}\boldsymbol{P}=\boldsymbol{0}, \qquad \mathscr{B}\times]t_{\mathrm{in}},t_{\mathrm{fin}}], \tag{12a}$$

$$\chi=\chi_{\mathrm{b}}, \qquad \partial^{\chi}_{\mathrm{D}}\mathscr{B}\times]t_{\mathrm{in}},t_{\mathrm{fin}}], \tag{12b}$$

$$\boldsymbol{P}\boldsymbol{N}=\boldsymbol{\tau}, \qquad \partial^{\chi}_{\mathrm{N}}\mathscr{B}\times]t_{\mathrm{in}},t_{\mathrm{fin}}], \tag{12c}$$

$$\tfrac{1}{3}J_{\boldsymbol{K}}\,\mathfrak{a}_\nu\,\operatorname{tr}(\boldsymbol{K}^{-1}\dot{\boldsymbol{K}})\boldsymbol{I}^{\mathrm{T}}+2J_{\boldsymbol{K}}\,\mathfrak{b}_\nu\boldsymbol{C}\,\operatorname{sym}[(\boldsymbol{K}^{-1}\dot{\boldsymbol{K}})\boldsymbol{C}^{-1}]=-\boldsymbol{H}+\boldsymbol{Z}, \qquad \mathscr{B}\times]t_{\mathrm{in}},t_{\mathrm{fin}}], \tag{12d}$$

$$2J_{\boldsymbol{K}}\mathfrak{c}_\nu\,\operatorname{skew}[(\boldsymbol{K}^{-1}\dot{\boldsymbol{K}})\boldsymbol{C}^{-1}]=\boldsymbol{0}, \qquad \mathscr{B}\times]t_{\mathrm{in}},t_{\mathrm{fin}}], \tag{12e}$$

$$\boldsymbol{K}(X,t_{\mathrm{in}})=\boldsymbol{K}_{\mathrm{in}}(X), \qquad \mathscr{B}. \tag{12f}$$

A preliminary version of the IBVP in (12a)–(12f), but without the separation of (12d) from (12e), and within a simplified framework, has been considered by [Licari 2021]. In fact, however, the presence of (12e) in our work constitutes a substantial change in the model, since it descends from isotropy and from the expression of $\boldsymbol{Z}$, as discussed in [Grillo and Di Stefano 2023a; 2023b], rather than being due to simplifying restrictions from the outset. Also, for the approach A2, the left-hand-side of (12d) is obtained by working out the constitutive expression of the dissipative part of the growth-conjugated, generalized internal force $\boldsymbol{Y}$, which reads (see [Grillo and Wittum 2010; Grillo et al. 2012; Licari 2021; Grillo and Di Stefano 2023a])

$$\begin{aligned}\boldsymbol{Y}_{\mathrm{d}}=\tfrac{1}{3}J_{\boldsymbol{K}}\,\mathfrak{a}_\nu\,\operatorname{tr}(\boldsymbol{K}^{-1}\dot{\boldsymbol{K}})\boldsymbol{I}^{\mathrm{T}}\\ +2J_{\boldsymbol{K}}\,\mathfrak{b}_\nu\boldsymbol{C}\,\operatorname{sym}[(\boldsymbol{K}^{-1}\dot{\boldsymbol{K}})\boldsymbol{C}^{-1}]+2J_{\boldsymbol{K}}\,\mathfrak{c}_\nu\boldsymbol{C}\,\operatorname{skew}[(\boldsymbol{K}^{-1}\dot{\boldsymbol{K}})\boldsymbol{C}^{-1}].\end{aligned} \tag{13}$$

Remark 2 (the chemo-mechanical coupling in the approach A2). In the approach A2 the growth law does not feature explicitly in the system (12a)–(12f) and, thus, the

chemo-mechanical coupling must be introduced through $\boldsymbol{Z}$ and, when required, through the coefficients $\mathfrak{a}_\nu$, $\mathfrak{b}_\nu$, and $\mathfrak{c}_\nu$, and the constitutive expressions of $\boldsymbol{P}$ and $\boldsymbol{H}$. Yet, if these dependences are disregarded, the approach A2 addresses the limit case of a "purely mechanical" growth, i.e., a growth that, in the jargon of [Epstein and Maugin 2000], is ascribable to the evolution of *"material inhomogeneities"*, but is independent of biological processes driven by nutrients (see also [Ambrosi and Guana 2007; Ambrosi and Guillou 2007]).

In the sequel, we assume that the chemo-mechanical coupling occurs essentially through $\boldsymbol{Z}$, as specified in Section 3.3, and we consider separately a situation in which also the coefficients $\mathfrak{a}_\nu$, $\mathfrak{b}_\nu$, and $\mathfrak{c}_\nu$ should be studied as functions of ω. Hence, we need to couple (12a)–(12f) with the initial and boundary value problem for ω reported in (4a)–(4d). It is worth noticing that, as explained in Remark 2 of [Grillo and Di Stefano 2023a], the linearity of the left-hand-side of (12d) allows us to compute the growth law a posteriori by simply taking the trace of (12d). In particular, by expressing $\boldsymbol{Z}$ as reported below in (17a)–(17e) (see [Grillo and Di Stefano 2023a]), we obtain

$$R_\gamma \equiv \operatorname{tr}(\boldsymbol{K}^{-1}\dot{\boldsymbol{K}}) = \frac{-\operatorname{tr}\boldsymbol{H}}{J_{\boldsymbol{K}}\{\mathfrak{a}_\nu + 2\mathfrak{b}_\nu\}} + \frac{\Gamma}{\mathfrak{a}_\nu + 2\mathfrak{b}_\nu} + \frac{Q_{\nu\ell} + 2Q_{\nu t}}{\mathfrak{a}_\nu + 2\mathfrak{b}_\nu}\|\operatorname{Grad}\omega\|_{\boldsymbol{C}^{-1}}. \quad (14)$$

An expression for R_γ similar to the one reported in (14), but without the last term and with Γ disregarding mass resorption, has been used in [Licari 2021]. Note also that other biological contexts in which a chemo-mechanical coupling is considered are the growth, the resorption and the remodeling of bone tissue (see, for example, [Giorgio et al. 2019]). Finally, we remark that, for a pioneering work leading to a growth law with the same rationale as (14), credit should be given to [Ambrosi and Guana 2007].

Remark 3 (on the influence of the Eshelby stress tensor). In the limit case of no appreciable mechanotransduction, which amounts to setting $\alpha = 0$ in (6), the influence of $\operatorname{tr}\boldsymbol{H}$ on $R_{\gamma(\mathrm{ph})}$ would be either null or only very indirect (for instance, through the coupling of the evolution of the nutrients with the deformation and, thus, with stress). However, even in such a situation, the influence of $\operatorname{tr}\boldsymbol{H}$ would still be effective in the approach A2, since $\frac{1}{3}(\operatorname{tr}\boldsymbol{H})\boldsymbol{I}^{\mathrm{T}}$ is the dual of $\boldsymbol{K}^{-1}\dot{\boldsymbol{K}}$ that describes, in general, the evolution of the mass of a body even when this is not necessarily associated with the availability of nutrients (see also [Ambrosi and Guana 2007]). In this respect, as anticipated by [Grillo and Di Stefano 2023a], this view recalls the one suggested by [Epstein and Maugin 2000] when they speak of growth in terms of evolution of *"material inhomogeneities"*.

3.3. ***Constitutive laws and generalized external force Z.*** We hypothesize that the medium under study is hyperelastic, and we define the Helmholtz free energy

density Ψ_{R} per unit volume of the medium's reference placement $\mathscr{B}$ as $\Psi_{\mathrm{R}} = \hat{\Psi}_{\mathrm{R}} \circ (\boldsymbol{F}, \boldsymbol{K}) = J_{\boldsymbol{K}}[\hat{\Psi}_{\nu} \circ \boldsymbol{F}_{\mathrm{e}}] = J_{\boldsymbol{K}} \Psi_{\nu}$, with $\boldsymbol{F}_{\mathrm{e}} = \boldsymbol{F}\boldsymbol{K}^{-1}$, where $\Psi_{\nu} := \hat{\Psi}_{\nu} \circ \boldsymbol{F}_{\mathrm{e}}$ is the Helmholtz free energy density per unit volume of the medium's natural state. We take $\hat{\Psi}_{\nu} \circ \boldsymbol{F}_{\mathrm{e}} \equiv \hat{\mathcal{W}}_{\nu} \circ (I_{1\mathrm{e}}, I_{2\mathrm{e}}, I_{3\mathrm{e}})$, where, following [Holmes and Mow 1990],

$$\hat{\mathcal{W}}_{\nu} \circ (I_{1\mathrm{e}}, I_{2\mathrm{e}}, I_{3\mathrm{e}}) = \alpha_0\big[\exp(\alpha_1[I_{1\mathrm{e}} - 3] + \alpha_2[I_{2\mathrm{e}} - 3] - \alpha_3 \log I_{3\mathrm{e}}) - 1\big], \quad (15)$$

and $I_{1\mathrm{e}}$, $I_{2\mathrm{e}}$, and $I_{3\mathrm{e}}$ are the three principal invariants of the elastic Cauchy–Green deformation tensor $\boldsymbol{C}_{\mathrm{e}} := \boldsymbol{F}_{\mathrm{e}}^{\mathrm{T}}.\boldsymbol{F}_{\mathrm{e}}$. Accordingly, the first Piola–Kirchhoff stress tensor $\boldsymbol{P}$ and the Eshelby tensor $\boldsymbol{H}$ read

$$\hat{\boldsymbol{P}} \circ (\boldsymbol{F}, \boldsymbol{K}) = 2J_{\boldsymbol{K}}[s_{1\mathrm{e}} + s_{2\mathrm{e}} I_{1\mathrm{e}}]\boldsymbol{g}\boldsymbol{F}\boldsymbol{B}_{\boldsymbol{K}} - 2J_{\boldsymbol{K}} s_{2\mathrm{e}} \boldsymbol{g}\boldsymbol{F}\boldsymbol{B}_{\boldsymbol{K}}\boldsymbol{C}\boldsymbol{B}_{\boldsymbol{K}} + 2J_{\boldsymbol{K}} s_{3\mathrm{e}} I_{3\mathrm{e}} \boldsymbol{g}\boldsymbol{F}\boldsymbol{C}^{-1},$$
$$\hat{\boldsymbol{H}} \circ (\boldsymbol{F}, \boldsymbol{K}) = [\hat{\Psi}_{\mathrm{R}} \circ (\boldsymbol{F}, \boldsymbol{K})]\boldsymbol{I}^{\mathrm{T}} - \boldsymbol{F}^{\mathrm{T}}[\hat{\boldsymbol{P}} \circ (\boldsymbol{F}, \boldsymbol{K})],$$

where we used the notation

$$s_{i\mathrm{e}} := \partial_{I_{i\mathrm{e}}} \hat{\mathcal{W}}_{\nu} \circ (I_{1\mathrm{e}}, I_{2\mathrm{e}}, I_{3\mathrm{e}}) \quad \text{for } i = 1, 2, 3, \qquad \text{and} \qquad \boldsymbol{B}_{\boldsymbol{K}} = \boldsymbol{K}^{-1}.\boldsymbol{K}^{-\mathrm{T}}. \quad (16)$$

The representation of the generalized external force $\boldsymbol{Z}$ has been recently discussed in [Grillo and Di Stefano 2023a] and, thus, we report here just its final definition:

$$\hat{\boldsymbol{Z}} \circ (\boldsymbol{F}, \boldsymbol{K}, \omega, \operatorname{Grad}\omega) := \tfrac{1}{3} J_{\boldsymbol{K}}[\hat{\Gamma} \circ (\boldsymbol{F}, \boldsymbol{K}, \omega)]\boldsymbol{I}^{\mathrm{T}} + \hat{\boldsymbol{Q}} \circ (\boldsymbol{F}, \boldsymbol{K}, \omega, \operatorname{Grad}\omega), \quad (17a)$$

$$\hat{\Gamma} \circ (\boldsymbol{F}, \boldsymbol{K}, \omega) := \kappa_{\mathrm{a}}[\hat{\Gamma}_{\mathrm{a}} \circ (\boldsymbol{F}, \boldsymbol{K}, \omega)] + \kappa_{\mathrm{r}}[\hat{\Gamma}_{\mathrm{r}} \circ \omega], \quad (17b)$$

$$\hat{\Gamma}_{\mathrm{a}} \circ (\boldsymbol{F}, \boldsymbol{K}, \omega) := \langle h_{\mathrm{a}} \circ \omega \rangle_{+} \left[1 - \frac{\alpha \, \langle \hat{\wp} \circ (\boldsymbol{F}, \boldsymbol{K}) \rangle_{+}}{\sigma_{\mathrm{c}} + \langle \hat{\wp} \circ (\boldsymbol{F}, \boldsymbol{K}) \rangle_{+}}\right], \quad (17c)$$

$$\hat{\Gamma}_{\mathrm{r}} \circ \omega := \langle h_{\mathrm{r}} \circ \omega \rangle_{+}, \quad (17d)$$

$$\hat{\boldsymbol{Q}} \circ (\boldsymbol{F}, \boldsymbol{K}, \omega, \operatorname{Grad}\omega) := J_{\boldsymbol{K}} Q_{\nu\mathrm{t}} \|\operatorname{Grad}\omega\|_{\boldsymbol{C}^{-1}} \boldsymbol{I}^{\mathrm{T}} + J_{\boldsymbol{K}} Q_{\nu\ell t} \frac{\operatorname{Grad}\omega \otimes \boldsymbol{C}^{-1} \operatorname{Grad}\omega}{\|\operatorname{Grad}\omega\|_{\boldsymbol{C}^{-1}}}, \quad (17e)$$

with $Q_{\nu\ell t} := Q_{\nu\ell} - Q_{\nu\mathrm{t}}$. Here, $\kappa_{\mathrm{a}} > 0$, $\kappa_{\mathrm{r}} < 0$, $Q_{\nu\ell}$, and $Q_{\nu\mathrm{t}}$ are assumed to be constant and represent stress-like quantities. In particular, κ_{a} and κ_{r} are identified through the relations $\kappa_{\mathrm{a}} = [a_{\nu} + 2b_{\nu}]\zeta_{\mathrm{a}}$ and $\kappa_{\mathrm{r}} = -[a_{\nu} + 2b_{\nu}]\zeta_{\mathrm{r}}$ (see [Grillo and Di Stefano 2023a]). Note that the same expression of $\boldsymbol{Z}$ is employed for both the approaches A1 and A2. Finally, we remark that, differently from (17e), the counterpart of our tensor $\boldsymbol{Q}$ used by [Licari 2021] is constant and defined to be deviatoric from the outset.

4. The approach A1 and the Cahn–Hilliard model

Recently, Grillo and Di Stefano [2023b] have reviewed Gurtin's formulation of the Cahn–Hilliard model for systems with variable mass [1996], and have put it into the context of growth, in the particular case in which the growth tensor $\boldsymbol{K}$ is assumed to be spherical. In such a situation, $\boldsymbol{K}$ can be written as $\boldsymbol{K} = {J_{\boldsymbol{K}}}^{1/3}\boldsymbol{I}$,

so that the identification $J_{\boldsymbol{K}} = \det \boldsymbol{K}$ holds true, and the variable $J_{\boldsymbol{K}}$ acquires the meaning of the order parameter of the considered theory of growth. Before going further, we remark that, in the present work, we adopt a geometric picture in which $\boldsymbol{K}$ is understood as a material tensor field, rather than as a two-point tensor field. This permits the use of the material identity tensor $\boldsymbol{I}$ instead of the shifter operator [Marsden and Hughes 1983]. In doing this, we refer to the theory of anelastic processes proposed by [Ciancio et al. 2008]. To match the constitutive requirements of the Cahn–Hilliard model, the theory of growth under study is formulated as *"a theory of grade one in"* $J_{\boldsymbol{K}}$ [Grillo and Di Stefano 2023b; 2023c]. In turn, this requires us to redefine the Helmholtz free energy density of the medium, which we take as

$$\hat{\Psi}_{\mathrm{R}} \circ (\boldsymbol{F}, J_{\boldsymbol{K}}, \operatorname{Grad} J_{\boldsymbol{K}}) = \hat{\Psi}_{\mathrm{R}0} \circ (\boldsymbol{F}, J_{\boldsymbol{K}}) + \hat{\mathcal{U}}_{\mathrm{R}} \circ J_{\boldsymbol{K}} + \tfrac{1}{2}\beta \, \|\operatorname{Grad} J_{\boldsymbol{K}}\|^2. \tag{18}$$

Here, $\hat{\Psi}_{\mathrm{R}0} \circ (\boldsymbol{F}, J_{\boldsymbol{K}}) := J_{\boldsymbol{K}}[\hat{\Psi}_{v0} \circ (\boldsymbol{F}, J_{\boldsymbol{K}})] \equiv J_{\boldsymbol{K}}[\hat{\mathcal{W}}_v \circ (I_{1\mathrm{e}}, I_{2\mathrm{e}}, I_{3\mathrm{e}})]$ is the strain energy density of the medium, with $\hat{\mathcal{W}}_v \circ (I_{1\mathrm{e}}, I_{2\mathrm{e}}, I_{3\mathrm{e}})$ given in (15), while $\beta > 0$ is a material parameter (see [Gurtin 1996]), and $\hat{\mathcal{U}}_{\mathrm{R}} \circ J_{\boldsymbol{K}} := J_{\boldsymbol{K}}[\hat{\mathcal{U}}_v \circ J_{\boldsymbol{K}}]$ is an energy density due to the interaction of $J_{\boldsymbol{K}}$ with itself, which we hypothesize to be of the type of a Lennard–Jones energy density, i.e.,

$$\hat{\mathcal{U}}_{\mathrm{R}} \circ J_{\boldsymbol{K}} := J_{\boldsymbol{K}}[\hat{\mathcal{U}}_v \circ J_{\boldsymbol{K}}] = 4\,\mathcal{U}_{\mathrm{R}0}\left[\left(\frac{1}{J_{\boldsymbol{K}}}\right)^{12} - \left(\frac{1}{J_{\boldsymbol{K}}}\right)^{6}\right], \quad \mathcal{U}_{\mathrm{R}0} := \alpha_0 \upsilon, \tag{19}$$

where $\mathcal{U}_{\mathrm{R}0}$ defines the depth of the well of the energy density $\hat{\mathcal{U}}_{\mathrm{R}} \circ J_{\boldsymbol{K}}$, and $\upsilon > 0$ is a nondimensional parameter introduced to modulate the magnitude of the elasticity constant α_0. Note that $\hat{\mathcal{U}}_{\mathrm{R}} \circ J_{\boldsymbol{K}}$ is "repulsive" until a global minimum is reached, and is "attractive" otherwise. We remark that the use of energy densities of the Lennard–Jones type is not new in the description of tumor growth and, indeed, within the biphasic framework, potential energy densities of this kind were used by [Ambrosi and Preziosi 2002; Byrne and Preziosi 2003; Agosti et al. 2018]. However, the functional forms of the energy densities adopted by these authors are different from the one employed in our work, which, being formulated within a monophasic framework, depends on $J_{\boldsymbol{K}}$.

The adaptation of [Gurtin 1996] to the growth problem investigated here yields the equations (see [Grillo and Di Stefano 2023b, for details])

$$\dot{J}_{\boldsymbol{K}} = -\operatorname{Div}\left[\mathfrak{M} \operatorname{Grad}\left(\frac{\mu_{\boldsymbol{K}}}{J_{\boldsymbol{K}}}\right)\right] + J_{\boldsymbol{K}} R_{\gamma(\mathrm{ph})}, \tag{20a}$$

$$\frac{\mu_{\boldsymbol{K}}}{J_{\boldsymbol{K}}} = \frac{z}{J_{\boldsymbol{K}}} - \kappa_v \frac{\dot{J}_{\boldsymbol{K}}}{J_{\boldsymbol{K}}} - \mathcal{E}_{J_{\boldsymbol{K}}} \Psi_{\mathrm{R}}, \tag{20b}$$

where $\mathfrak{M}$ is the material mobility tensor of the medium, and, in general, it is a second-order, symmetric, positive semidefinite, "contravariant" tensor field. In this

work, $\mathfrak{M}$ is assumed to be spherical, so that the definition $\mathfrak{M} := \mathfrak{M}\boldsymbol{G}^{-1}$ applies, and $\mathfrak{M}$, which is the scalar mobility of the system, is assumed to be a strictly positive scalar field, unless when it is taken to be null for comparison with the case of no diffusion. Consequently, $\mathfrak{M}$ turns out to be positive definite for $\mathfrak{M} > 0$. Equations (20a) and (20b) generalize the approach A1 presented in Section 3.1 to a theory of grade one in the anelastic variable, i.e., the growth tensor, here represented by $J_{\boldsymbol{K}}$. In (20a) and (20b), $\mu_{\boldsymbol{K}}$ is the Lagrange multiplier associated with the mass balance (20a), suitably interpreted as a constraint; z is the scalar-valued generalized external force power-conjugated to $J_{\boldsymbol{K}}^{-1}\dot{J}_{\boldsymbol{K}}$ (here it is taken as $z = \frac{1}{3}\operatorname{tr}\boldsymbol{Z}$, with $\boldsymbol{Z}$ given in (17a)–(17e)); $\mathcal{E}_{J_{\boldsymbol{K}}}\Psi_{\mathrm{R}}$ is the Euler-Lagrange operator, which, granted (18), reads

$$\begin{aligned}\mathcal{E}_{J_{\boldsymbol{K}}}\Psi_{\mathrm{R}} &= \frac{\partial\hat{\Psi}_{\mathrm{R}}}{\partial J_{\boldsymbol{K}}}\circ(\boldsymbol{F}, J_{\boldsymbol{K}}, \operatorname{Grad} J_{\boldsymbol{K}}) - \operatorname{Div}\left[\frac{\partial\hat{\Psi}_{\mathrm{R}}}{\partial \operatorname{Grad} J_{\boldsymbol{K}}}\circ(\boldsymbol{F}, J_{\boldsymbol{K}}, \operatorname{Grad} J_{\boldsymbol{K}})\right]\\ &= J_{\boldsymbol{K}}^{-1}[\hat{\mathfrak{h}}\circ(\boldsymbol{F}, J_{\boldsymbol{K}})] - \operatorname{Div}[\beta\boldsymbol{G}^{-1}\operatorname{Grad} J_{\boldsymbol{K}}],\end{aligned} \tag{21}$$

where we have set

$$\begin{aligned}\mathfrak{h} &:= \hat{\mathfrak{h}}\circ(\boldsymbol{F}, J_{\boldsymbol{K}}) \equiv J_{\boldsymbol{K}}\left[\frac{\partial\hat{\Psi}_{\mathrm{R}}}{\partial J_{\boldsymbol{K}}}\circ(\boldsymbol{F}, J_{\boldsymbol{K}}, \operatorname{Grad} J_{\boldsymbol{K}})\right]\\ &= J_{\boldsymbol{K}}\left[\frac{\partial\hat{\Psi}_{\mathrm{R0}}}{\partial J_{\boldsymbol{K}}}\circ(\boldsymbol{F}, J_{\boldsymbol{K}}) + \frac{\partial\hat{\mathcal{U}}_{\mathrm{R}}}{\partial J_{\boldsymbol{K}}}\circ J_{\boldsymbol{K}}\right]\\ &= J_{\boldsymbol{K}}\left\{\hat{\Psi}_{\nu 0}\circ(\boldsymbol{F}, J_{\boldsymbol{K}}) - \sum_{i=1}^{3}\frac{2i}{3}[\hat{s}_{i\mathrm{e}}\circ(\boldsymbol{F}, J_{\boldsymbol{K}})][\hat{I}_{i\mathrm{e}}\circ(\boldsymbol{F}, J_{\boldsymbol{K}})] + \frac{\partial\hat{\mathcal{U}}_{\mathrm{R}}}{\partial J_{\boldsymbol{K}}}\circ J_{\boldsymbol{K}}\right\}\end{aligned} \tag{22}$$

to indicate the scalar Eshelby stress of the theory, generated by $\hat{\Psi}_{\mathrm{R0}}\circ(\boldsymbol{F}, J_{\boldsymbol{K}})$ and $\hat{\mathcal{U}}_{\mathrm{R}}\circ J_{\boldsymbol{K}}$ (see also [Crevacore et al. 2019]). To obtain (22), we have set $\hat{s}_{i\mathrm{e}}\circ(\boldsymbol{F}, J_{\boldsymbol{K}}) \equiv s_{i\mathrm{e}} = \partial_{I_{i\mathrm{e}}}\hat{\mathcal{W}}_{\nu}\circ(I_{1\mathrm{e}}, I_{2\mathrm{e}}, I_{3\mathrm{e}})$, for $i = 1, 2, 3$, and we have written $I_{i\mathrm{e}}$ as a function of $\boldsymbol{F}$ and $J_{\boldsymbol{K}}$, for all $i = 1, 2, 3$, that is, $I_{i\mathrm{e}} \equiv \hat{I}_{i\mathrm{e}}\circ(\boldsymbol{F}, J_{\boldsymbol{K}}) = J_{\boldsymbol{K}}^{-2i/3}I_i$, with I_i being the i-th principal invariant of $\boldsymbol{C}$, so that we find $\partial_{J_{\boldsymbol{K}}}\hat{I}_{i\mathrm{e}}\circ(\boldsymbol{F}, J_{\boldsymbol{K}}) = -(2i/3)J_{\boldsymbol{K}}^{-1}I_{i\mathrm{e}}$.

With all these premises, we can recast (20a) and (20b) in the form

$$-\operatorname{Div}\left[\mathfrak{M}\boldsymbol{G}^{-1}\operatorname{Grad}\left(\frac{\mu_{\boldsymbol{K}}}{J_{\boldsymbol{K}}}\right)\right] = \dot{J}_{\boldsymbol{K}} - J_{\boldsymbol{K}}R_{\gamma(\mathrm{ph})}, \tag{23a}$$

$$\kappa_{\nu}\frac{\dot{J}_{\boldsymbol{K}}}{J_{\boldsymbol{K}}} - \operatorname{Div}[\beta\boldsymbol{G}^{-1}\operatorname{Grad} J_{\boldsymbol{K}}] = \frac{z}{J_{\boldsymbol{K}}} - \frac{\mathfrak{h}}{J_{\boldsymbol{K}}} - \frac{\mu_{\boldsymbol{K}}}{J_{\boldsymbol{K}}}, \tag{23b}$$

so that (23a), which reformulates the mass balance law, i.e., the constraint of the present theory, is a generalized Poisson equation for the Lagrange multiplier $\mu_{\boldsymbol{K}}$, whereas (23b), which is the dynamic equation, becomes a diffusion-reaction equation for $J_{\boldsymbol{K}}$. Clearly, differently from the approach A1 of grade zero in the growth tensor, in which the gradient of $\boldsymbol{K}$ is not regarded as a constitutive variable of the

model (see Section 3.1), boundary conditions for both $\mu_{\boldsymbol{K}}$ and $J_{\boldsymbol{K}}$ are required in addition to the initial condition for $J_{\boldsymbol{K}}$. Here, we choose

$$\left[-\mathfrak{M}\boldsymbol{G}^{-1}\,\mathrm{Grad}\left(\frac{\mu_{\boldsymbol{K}}}{J_{\boldsymbol{K}}}\right)\right]\boldsymbol{N}=0 \quad \text{on } \partial_{\mathrm{N}}^{\mu_{\boldsymbol{K}}/J_{\boldsymbol{K}}}\mathscr{B}, \tag{24a}$$

$$[-\beta\boldsymbol{G}^{-1}\,\mathrm{Grad}\,J_{\boldsymbol{K}}]\boldsymbol{N}=0 \quad \text{on } \partial_{\mathrm{N}}^{J_{\boldsymbol{K}}}\mathscr{B}, \tag{24b}$$

$$J_{\boldsymbol{K}}(X,t_{\mathrm{in}})=J_{\boldsymbol{K}\mathrm{in}}(X) \quad \text{in } \mathscr{B}, \tag{24c}$$

where $\partial_{\mathrm{N}}^{\mu_{\boldsymbol{K}}/J_{\boldsymbol{K}}}\mathscr{B}$ and $\partial_{\mathrm{N}}^{J_{\boldsymbol{K}}}\mathscr{B}$ denote the portions of the boundary of $\mathscr{B}$ on which Neumann conditions are imposed for $\mu_{\boldsymbol{K}}/J_{\boldsymbol{K}}$ and $J_{\boldsymbol{K}}$, respectively. Note that, in the case studied here, (24b) transforms (24a) into a Neumann condition for $\mu_{\boldsymbol{K}}$, so that the boundary portion $\partial_{\mathrm{N}}^{\mu_{\boldsymbol{K}}/J_{\boldsymbol{K}}}\mathscr{B}$ can be rewritten as $\partial_{\mathrm{N}}^{\mu_{\boldsymbol{K}}}\mathscr{B}$.

Equations (23a), (23b), and (24a)–(24c) must be studied together with the linear momentum balance law (8a) and the boundary conditions (8b) and (8c), and with the initial and boundary value problem (4a)–(4d) for the nutrients' mass fraction. It should be emphasized that (4a) must be solved in the form

$$J_{\boldsymbol{K}}\varrho_{\nu}\dot{\omega}-\mathrm{Div}(J_{\boldsymbol{K}}\varrho_{\nu}\boldsymbol{D}\,\mathrm{Grad}\,\omega)=-J_{\boldsymbol{K}}\varrho_{\nu}r_{\mathrm{n}}\omega-\varrho_{\nu}\dot{J}_{\boldsymbol{K}}\omega, \tag{25}$$

because it is no longer true that $\dot{J}_{\boldsymbol{K}}$ equals $J_{\boldsymbol{K}}R_{\gamma(\mathrm{ph})}$, since the mass balance law is given by (23a). While (8d) and (8e) are disregarded by the present model, since taking the growth tensor to be spherical rules out the deviatoric components of the generalized forces dual to its variations, (23a) and (23b) replace (8f) and (10), respectively, while the initial condition (24c) replaces the one supplied in (8g).

We remark that, in the approach A1 of grade zero in the growth tensor, i.e., the one in which no spatial derivative of the growth tensor is accounted for (see Section 3.1), the Lagrange multiplier $\mu_{\boldsymbol{K}}$ can be computed either through (8f), i.e., the constraint, by means of the Schur complement technique, or *separately* from the problem (8a)–(8g), as we in fact do in Section 3.1. However, within the theory of grade one in $J_{\boldsymbol{K}}$ described in the present section, it is not possible to decouple the equation for $\mu_{\boldsymbol{K}}$ from the rest of the problem. In addition, it is more convenient to use the constraint, written as (23a), as the "equation for $\mu_{\boldsymbol{K}}$", and (23b) as the "equation for $J_{\boldsymbol{K}}$".

5. A mixed approach

The rationale for developing a "mixed" approach is that the constitutive assumption on $\boldsymbol{Y}_{\mathrm{d}}$ supplied in (13) is generally inconsistent with the growth law for R_{γ} obtained in (14) when the latter one is required to be zero on phenomenological grounds, as could be the case for $\omega=\omega_{\mathrm{cr}}$ (see [Mascheroni et al. 2016; 2018]). Therefore, the condition $\omega=\omega_{\mathrm{cr}}$ imposes a change of paradigm, which amounts to prescribing $\mathrm{tr}(\boldsymbol{K}^{-1}\dot{\boldsymbol{K}})$ through a constraint [Grillo et al. 2019b; Grillo and Di Stefano 2023b; Grillo and Di Stefano 2023c]. This, in turn, means that the force conjugated with

this generalized velocity, i.e., $\frac{1}{3}\operatorname{tr}(\boldsymbol{Y}_{\mathrm{d}})$, has to be *constitutively indeterminate* in this case, whereas it is constitutively determinate for $\omega \neq \omega_{\mathrm{cr}}$. Hence, in light of these considerations, we write:

(1) If $\omega = \omega_{\mathrm{cr}}$, then set

$$R_\gamma \equiv R_{\gamma(\mathrm{ph})} = 0 \tag{26}$$

and solve

(a) the IBVPs (8a)–(8g) and (4a)–(4d) for χ, $\boldsymbol{K}$, and ω;

(b) (10) for $\mu_{\boldsymbol{K}}$.

(2) If $\omega \neq \omega_{\mathrm{cr}}$, then solve the IBVPs (12a)–(12f) and (4a)–(4d) for χ, $\boldsymbol{K}$, and ω, with $\mathfrak{a}_\nu \equiv \hat{\mathfrak{a}}_\nu \circ \omega$ defined as a function of the nutrients' mass fraction.

In particular, for the case under study, upon introducing the auxiliary function

$$h \circ \omega := \langle h_{\mathrm{a}} \circ \omega \rangle_+ + \langle h_{\mathrm{r}} \circ \omega \rangle_+ \quad \text{such that } h \circ \omega_{\mathrm{cr}} = 0, \tag{27}$$

the generalized viscosity $\hat{\mathfrak{a}}_\nu \circ \omega$, for $\omega \neq \omega_{\mathrm{cr}}$, is prescribed to be

$$\hat{\mathfrak{a}}_\nu \circ \omega := \frac{a_\nu}{h \circ \omega} = \begin{cases} \dfrac{a_\nu}{h_{\mathrm{a}} \circ \omega} & \text{if } \omega > \omega_{\mathrm{cr}}, \\ \dfrac{a_\nu}{h_{\mathrm{r}} \circ \omega} & \text{if } \omega < \omega_{\mathrm{cr}}, \end{cases} \tag{28}$$

with constant $a_\nu > 0$, so that it diverges positively in the limit $\omega \to \omega_{\mathrm{cr}}$, while it is undefined for $\omega = \omega_{\mathrm{cr}}$. Note that, for $\omega \neq \omega_{\mathrm{cr}}$, and with this definition of $\mathfrak{a}_\nu \equiv \hat{\mathfrak{a}}_\nu \circ \omega$, the growth law predicted by (14) becomes

$$\begin{aligned} R_\gamma &\equiv \operatorname{tr}(\boldsymbol{K}^{-1}\dot{\boldsymbol{K}}) \\ &= \frac{-\operatorname{tr}[\hat{\boldsymbol{H}} \circ (\boldsymbol{F}, \boldsymbol{K})]}{J_{\boldsymbol{K}}\{[\hat{\mathfrak{a}}_\nu \circ \omega] + 2b_\nu\}} + \frac{\operatorname{tr}[\hat{\boldsymbol{Z}} \circ (\boldsymbol{F}, \boldsymbol{K}, \omega, \operatorname{Grad}\omega)]}{J_{\boldsymbol{K}}\{[\hat{\mathfrak{a}}_\nu \circ \omega] + 2b_\nu\}} \\ &= \frac{-[h \circ \omega]\operatorname{tr}[\hat{\boldsymbol{H}} \circ (\boldsymbol{F}, \boldsymbol{K})]}{J_{\boldsymbol{K}}\{a_\nu + 2b_\nu[h \circ \omega]\}} + \frac{[h \circ \omega]\operatorname{tr}[\hat{\boldsymbol{Z}} \circ (\boldsymbol{F}, \boldsymbol{K}, \omega, \operatorname{Grad}\omega)]}{J_{\boldsymbol{K}}\{a_\nu + 2b_\nu[h \circ \omega]\}}, \end{aligned} \tag{29}$$

and it can be prolongated to zero for $\omega \to \omega_{\mathrm{cr}}$, thereby reobtaining the approach A1.

6. Benchmark test and numerical results

We assume the initial placement and the current placement at time $t \in [t_{\mathrm{in}}, t_{\mathrm{fin}}]$ of the medium have shapes $\mathscr{B} = S \times]-L_{\mathrm{in}}/2, L_{\mathrm{in}}/2[$ and $\mathscr{B}_t = S \times]-L(t)/2, L(t)/2[$, respectively. Here, S is the time-independent, circular cross section of the cylinder representing the breast duct, with radius R_{in}, while L_{in} and $L(t)$ are the tumor's initial and current lengths. The initial placement of the medium is taken coincident with its reference placement, and the latter is hypothesized to be in the natural state both for the approach A1 (but not for the Cahn–Hilliard model) and for the approach A2. By endowing $\mathscr{B}$ and $\mathscr{B}_t$ with two systems of cylindrical coordinates, we can write, with a

parameter	unit	value	equation	reference
ζ_a	[1/s]	$1.343 \cdot 10^{-6}$	(6)	[Chaplain et al. 2006]
ζ_r	[1/s]	$1.150 \cdot 10^{-8}$	(6)	[Chaplain et al. 2006]
ω_{cr}	[−]	$1.000 \cdot 10^{-3}$	(7)	[Di Stefano et al. 2018]
ω_{env}	[−]	$7.000 \cdot 10^{-3}$	(7)	[Di Stefano et al. 2018]
r_n	[1/s]	$3.000 \cdot 10^{-7}$	(1) and (2)	[Casciari et al. 1992]
α	[−]	$7.138 \cdot 10^{-1}$	(6)	[Mascheroni et al. 2016]
σ_c	[Pa]	$1.541 \cdot 10^{3}$	(6)	[Mascheroni et al. 2016]
α_0	[Pa]	$5.300 \cdot 10^{4}$	(15)	[Mascheroni et al. 2018]
α_1	[−]	$5.090 \cdot 10^{-1}$	(15)	[Mascheroni et al. 2018]
α_2	[−]	$2.450 \cdot 10^{-1}$	(15)	[Mascheroni et al. 2018]
α_3	[−]	1	(15)	[Mascheroni et al. 2018]
d_{0R}	[m^2/s]	$3.200 \cdot 10^{-9}$	–	[Holmes and Mow 1990]
$Q_{\nu t}$	[N/m]	$0.500 \cdot 10^{-3}$	(17e)	–
$Q_{\nu \ell}$	[N/m]	$1.000 \cdot 10^{-3}$	(17e)	–
a_ν	[Pa s]	$2.000 \cdot 10^{8}$	–	–
b_ν	[Pa s]	$1.000 \cdot 10^{8}$	–	–
$\mathfrak{M}$	[m^2/Pa s]	$2.000 \cdot 10^{8}$	(23a)	–
β	[N]	$\alpha_0 L_{in}^2$	(23b)	–

Table 1. Parameters used in the numerical simulations. We set $L_{in} = 1.000\,\text{cm}$, $\varrho_\nu = 1000\,\text{kg/m}^3$, $\kappa_\nu = a_\nu + 2b_\nu$, $\upsilon = 10$ and $\epsilon = 0.008$. The last six parameters are introduced in the present work. We recall that k_a and k_r are obtained by $k_a = [a_\nu + 2b_\nu]\zeta_a$ and $k_r = -[a_\nu + 2b_\nu]\zeta_r$.

slight abuse of notation, $X = (R, \Theta, \Xi)$ and $x = (r, \theta, \xi)$ for the coordinate representations of the generic points $X \in \mathscr{B}$ and $x \in \mathscr{B}_t$ in terms of radial, circumferential, and axial coordinates, respectively. The particularly simple geometry and the symmetries assumed in the sequel lend themselves well to benchmarking, and, indeed, they have been used by many authors for this purpose. Here, we are taking inspiration from [Ambrosi and Mollica 2002], in which this setting was originally formulated for a very fundamental growth problem, and we are modifying some previous studies available in the literature [Di Stefano et al. 2018; Grillo et al. 2019b; Licari 2021].

In light of the above discussion, we suppose that all the dependent physical variables of interest depend exclusively on the axial coordinate and time. Hence, the motion of the system and the nutrients' mass fraction can be recast in the form

$$\chi(R, \Theta, \Xi, t) = (R, \Theta, \Xi + \bar{u}(\Xi, t)), \tag{30a}$$

$$\omega(R, \Theta, \Xi, t) \equiv \bar{\omega}(\Xi, t), \tag{30b}$$

where $\bar{u}$ describes the field of axial displacement of the tumor, and $\boldsymbol{F}(R, \Theta, \Xi, t) \equiv \bar{\boldsymbol{F}}(\Xi, t)$ and $\operatorname{Grad}\omega(R, \Theta, \Xi, t)$ are represented by

$$[\bar{\boldsymbol{F}}(\Xi, t)] = \operatorname{diag}\{1, 1, 1 + \bar{u}_{,\Xi}(\Xi, t)\}, \quad \bar{u}_{,\Xi}(\Xi, t) \equiv \partial_{\Xi}\bar{u}(\Xi, t), \tag{31a}$$

$$[\operatorname{Grad}\omega(R, \Theta, \Xi, t)] = \begin{bmatrix} 0 & 0 & \bar{\omega}_{,\Xi}(\Xi, t) \end{bmatrix}. \tag{31b}$$

In addition, $\boldsymbol{K}(R, \Theta, \Xi, t) \equiv \bar{\boldsymbol{K}}(\Xi, t)$, $\boldsymbol{P}(R, \Theta, \Xi, t) \equiv \bar{\boldsymbol{P}}(\Xi, t)$, $\boldsymbol{H}(R, \Theta, \Xi, t) \equiv \bar{\boldsymbol{H}}(\Xi, t)$, and $\boldsymbol{Z}(R, \Theta, \Xi, t) \equiv \bar{\boldsymbol{Z}}(\Xi, t)$ have all diagonal matrix representation, i.e.,

$$[\bar{\boldsymbol{K}}(\Xi, t)] = \operatorname{diag}\{\bar{K}^{R}{}_{R}(\Xi, t), \bar{K}^{\Theta}{}_{\Theta}(\Xi, t), \bar{K}^{\Xi}{}_{\Xi}(\Xi, t)\}, \tag{32a}$$

$$[\bar{\boldsymbol{P}}(\Xi, t)] = \operatorname{diag}\{\bar{P}_{r}{}^{R}(\Xi, t), \bar{P}_{\theta}{}^{\Theta}(\Xi, t), \bar{P}_{\xi}{}^{\Xi}(\Xi, t)\}, \tag{32b}$$

$$[\bar{\boldsymbol{H}}(\Xi, t)] = \operatorname{diag}\{\bar{H}_{R}{}^{R}(\Xi, t), \bar{H}_{\Theta}{}^{\Theta}(\Xi, t), \bar{H}_{\Xi}{}^{\Xi}(\Xi, t)\}, \tag{32c}$$

$$[\bar{\boldsymbol{Z}}(\Xi, t)] = \operatorname{diag}\{\bar{Z}_{R}{}^{R}(\Xi, t), \bar{Z}_{\Theta}{}^{\Theta}(\Xi, t), \bar{Z}_{\Xi}{}^{\Xi}(\Xi, t)\}. \tag{32d}$$

We remark that, differently from what has been done by [Ambrosi and Mollica 2002; Di Stefano et al. 2018; Grillo et al. 2019b; Ramírez-Torres et al. 2021], $\boldsymbol{K}$ is not assumed to be spherical, although it is diagonal (see also [Licari 2021], in which, however, the evolution of the nutrients is not solved, a different definition of $\boldsymbol{Z}$ is presumed, and the approach A1 is not investigated). In this respect, we recall that, as anticipated above, in this work we consider $\boldsymbol{K}$ as a mixed, rather than two-point, material tensor field. Finally, we introduce the notation

$$J_{\boldsymbol{K}}(R, \Theta, \Xi, t) \equiv \bar{\jmath}_{\boldsymbol{K}}(\Xi, t), \tag{33a}$$

$$\operatorname{tr}\{[\boldsymbol{K}^{-1}(R, \Theta, \Xi, t)]\,[\dot{\boldsymbol{K}}(R, \Theta, \Xi, t)]\} \equiv \bar{\Lambda}_{\mathrm{vol}}(\Xi, t), \tag{33b}$$

$$R_{\gamma(\mathrm{ph})}(R, \Theta, \Xi, t) \equiv \bar{R}_{\gamma(\mathrm{ph})}(\Xi, t), \tag{33c}$$

$$\mu_{\boldsymbol{K}}(R, \Theta, \Xi, t) \equiv \bar{\mu}_{\boldsymbol{K}}(\Xi, t). \tag{33d}$$

With respect to the chosen benchmark test, the unknowns of the problem are

$$\bar{u}, \bar{K}^{R}{}_{R}, \bar{K}^{\Theta}{}_{\Theta}, \bar{K}^{\Xi}{}_{\Xi}, \bar{\mu}_{\boldsymbol{K}}, \bar{\mu}_{\mathfrak{T}}, \bar{\mathcal{Y}}_{\mathrm{u}} - \bar{\mathcal{Z}}, \bar{\omega} \quad \text{for the approach A1,} \tag{34a}$$

$$\bar{u}, \bar{K}^{R}{}_{R}, \bar{K}^{\Theta}{}_{\Theta}, \bar{K}^{\Xi}{}_{\Xi}, \bar{\omega} \quad \text{for the approach A2,} \tag{34b}$$

$$\bar{u}, \bar{\jmath}_{\boldsymbol{K}}, \bar{\mu}_{\boldsymbol{K}}, \bar{\omega} \quad \text{for the Cahn–Hilliard model,} \tag{34c}$$

where $\bar{\mu}_{\mathfrak{T}}(\Xi, t) \equiv \mu_{\mathfrak{T}}(R, \Theta, \Xi, t)$, $\bar{\mathcal{Y}}_{\mathrm{u}}(\Xi, t) \equiv \mathcal{Y}_{\mathrm{u}}(R, \Theta, \Xi, t)$, and $\bar{\mathcal{Z}}(\Xi, t) \equiv \mathcal{Z}(R, \Theta, \Xi, t)$. From here on, we make the further assumption that the coefficients $\mathfrak{a}_{\nu}$, $\mathfrak{b}_{\nu}$, and $\mathfrak{c}_{\nu}$, which, in general, may depend on the nutrients' mass fraction, are replaced with the constants a_{ν}, b_{ν}, and c_{ν} (see Table 1). Note that, in this work, $\bar{\mathcal{Y}}_{\mathrm{u}} - \bar{\mathcal{Z}}$ is regarded as *one* unknown.

6.1. ***Summary of the model equations.*** In this section, we summarize the IBVPs for all the approaches considered in this work.

Approach A1. In this approach, we consider

$$\bar{P}_{\xi}{}^{\Xi}{}_{,\Xi} = 0, \tag{35a}$$

$$\frac{\dot{\bar{K}}^{R}{}_{R}}{\bar{K}^{R}{}_{R}} + \frac{\dot{\bar{K}}^{\Theta}{}_{\Theta}}{\bar{K}^{\Theta}{}_{\Theta}} + \frac{\dot{\bar{K}}^{\Xi}{}_{\Xi}}{\bar{K}^{\Xi}{}_{\Xi}} = \bar{R}_{\gamma(\mathrm{ph})}, \tag{35b}$$

$$2\bar{\jmath}_{\boldsymbol{K}} b_{\nu}\left[\frac{2}{3}\frac{\dot{\bar{K}}^{\Theta}{}_{\Theta}}{\bar{K}^{\Theta}{}_{\Theta}} - \left(\frac{\dot{\bar{K}}^{R}{}_{R}}{\bar{K}^{R}{}_{R}} + \frac{\dot{\bar{K}}^{\Xi}{}_{\Xi}}{\bar{K}^{\Xi}{}_{\Xi}}\right)\right] = [-\mathrm{dev}\,\bar{\boldsymbol{H}} + \mathrm{dev}\,\bar{\boldsymbol{Z}}]_{\Theta}{}^{\Theta}, \tag{35c}$$

$$2\bar{\jmath}_{\boldsymbol{K}} b_{\nu}\left[\frac{2}{3}\frac{\dot{\bar{K}}^{\Xi}{}_{\Xi}}{\bar{K}^{\Xi}{}_{\Xi}} - \left(\frac{\dot{\bar{K}}^{R}{}_{R}}{\bar{K}^{R}{}_{R}} + \frac{\dot{\bar{K}}^{\Theta}{}_{\Theta}}{\bar{K}^{\Theta}{}_{\Theta}}\right)\right] = [-\mathrm{dev}\,\bar{\boldsymbol{H}} + \mathrm{dev}\,\bar{\boldsymbol{Z}}]_{\Xi}{}^{\Xi}, \tag{35d}$$

$$\bar{\jmath}_{\boldsymbol{K}}\dot{\bar{\omega}} - (\bar{\jmath}_{\boldsymbol{K}}\bar{D}^{\Xi\Xi}\bar{\omega}_{,\Xi})_{,\Xi} = -\bar{\jmath}_{\boldsymbol{K}} r_{\mathrm{n}}\bar{\omega} - \bar{\jmath}_{\boldsymbol{K}}\bar{\omega}\,\bar{R}_{\gamma(\mathrm{ph})}, \tag{35e}$$

with $\bar{D}^{\Xi\Xi}(\Xi, t) \equiv D^{\Xi\Xi}(R, \Theta, \Xi, t)$. We compute $\bar{\mu}_{\boldsymbol{K}}$, $\bar{\mu}_{\mathfrak{T}}$, and $\bar{\mathfrak{Y}}_{\mathrm{u}} - \bar{\mathcal{Z}}$ as

$$\begin{aligned}\bar{\mu}_{\boldsymbol{K}} = {} & \tfrac{1}{3}[\bar{Z}_{R}{}^{R} + \bar{Z}_{\Theta}{}^{\Theta} + \bar{Z}_{\Xi}{}^{\Xi}] \\ & - \tfrac{1}{3}[\bar{H}_{R}{}^{R} + \bar{H}_{\Theta}{}^{\Theta} + \bar{H}_{\Xi}{}^{\Xi}] - \tfrac{1}{3}\bar{\jmath}_{\boldsymbol{K}}[a_{\nu} + 2b_{\nu}]\bar{R}_{\gamma(\mathrm{ph})},\end{aligned} \tag{36a}$$

$$\bar{\mu}_{\mathfrak{T}} = -\bar{\mu}_{\boldsymbol{K}}\bar{R}_{\gamma(\mathrm{ph})}, \tag{36b}$$

$$\bar{\mathfrak{Y}}_{\mathrm{u}} - \bar{\mathcal{Z}} = -\bar{\mu}_{\mathfrak{T}}, \tag{36c}$$

decoupled from (35a)–(35e).

For the Cahn–Hilliard model, we have

$$\bar{P}_{\xi}{}^{\Xi}{}_{,\Xi} = 0, \tag{37a}$$

$$-\left[\mathfrak{M}\left(\frac{\bar{\mu}_{\boldsymbol{K}}}{\bar{\jmath}_{\boldsymbol{K}}}\right)_{,\Xi}\right]_{,\Xi} = \dot{\bar{\jmath}}_{\boldsymbol{K}} - \bar{\jmath}_{\boldsymbol{K}}\bar{R}_{\gamma(\mathrm{ph})}, \tag{37b}$$

$$\frac{\kappa_{\nu}\dot{\bar{\jmath}}_{\boldsymbol{K}}}{\bar{\jmath}_{\boldsymbol{K}}} - [\beta\bar{\jmath}_{\boldsymbol{K}}{}_{,\Xi}]_{,\Xi} = \frac{\bar{z} - \bar{\mathfrak{h}} - \bar{\mu}_{\boldsymbol{K}}}{\bar{\jmath}_{\boldsymbol{K}}}, \tag{37c}$$

$$\bar{\jmath}_{\boldsymbol{K}}\dot{\bar{\omega}} - (\bar{\jmath}_{\boldsymbol{K}}\bar{D}^{\Xi\Xi}\bar{\omega}_{,\Xi})_{,\Xi} = -\bar{\jmath}_{\boldsymbol{K}} r_{\mathrm{n}}\bar{\omega} - \dot{\bar{\jmath}}_{\boldsymbol{K}}\bar{\omega}, \tag{37d}$$

with $\bar{z}(\Xi, t) = z(R, \Theta, \Xi, t)$ and $\bar{\mathfrak{h}}(\Xi, t) = \mathfrak{h}(R, \Theta, \Xi, t)$. The "standard" model is obtained by setting $\mathfrak{M} = 0$, $\beta = 0$ and $\upsilon = 0$ (see (37b), (37c) and (19), respectively).

Approach A2. In this approach, we consider

$$\bar{P}_{\xi}{}^{\Xi}{}_{,\Xi} = 0, \tag{38a}$$

$$\bar{\jmath}_{\boldsymbol{K}}\left[\left(\frac{a_{\nu}}{3} + 2b_{\nu}\right)\frac{\dot{\bar{K}}^{R}{}_{R}}{\bar{K}^{R}{}_{R}} + \frac{a_{\nu}}{3}\left(\frac{\dot{\bar{K}}^{\Theta}{}_{\Theta}}{\bar{K}^{\Theta}{}_{\Theta}} + \frac{\dot{\bar{K}}^{\Xi}{}_{\Xi}}{\bar{K}^{\Xi}{}_{\Xi}}\right)\right] = -\bar{H}_{R}{}^{R} + \bar{Z}_{R}{}^{R}, \tag{38b}$$

$$\bar{\jmath}_{\boldsymbol{K}}\left[\left(\frac{a_{\nu}}{3} + 2b_{\nu}\right)\frac{\dot{\bar{K}}^{\Theta}{}_{\Theta}}{\bar{K}^{\Theta}{}_{\Theta}} + \frac{a_{\nu}}{3}\left(\frac{\dot{\bar{K}}^{R}{}_{R}}{\bar{K}^{R}{}_{R}} + \frac{\dot{\bar{K}}^{\Xi}{}_{\Xi}}{\bar{K}^{\Xi}{}_{\Xi}}\right)\right] = -\bar{H}_{\Theta}{}^{\Theta} + \bar{Z}_{\Theta}{}^{\Theta}, \tag{38c}$$

$$\bar{J}_{\boldsymbol{K}}\left[\left(\frac{a_v}{3}+2b_v\right)\frac{\dot{\bar{K}}^{\Xi}{}_{\Xi}}{\bar{K}^{\Xi}{}_{\Xi}}+\frac{a_v}{3}\left(\frac{\dot{\bar{K}}^{R}{}_{R}}{\bar{K}^{R}{}_{R}}+\frac{\dot{\bar{K}}^{\Theta}{}_{\Theta}}{\bar{K}^{\Theta}{}_{\Theta}}\right)\right]=-\bar{H}_{\Xi}{}^{\Xi}+\bar{Z}_{\Xi}{}^{\Xi}, \tag{38d}$$

$$\bar{J}_{\boldsymbol{K}}\dot{\bar{\omega}}-(\bar{J}_{\boldsymbol{K}}\bar{D}^{\Xi\Xi}\,\bar{\omega}_{,\Xi})_{,\Xi}=-\bar{J}_{\boldsymbol{K}}r_{\mathrm{n}}\bar{\omega}-\bar{J}_{\boldsymbol{K}}\bar{\omega}\,\bar{\Lambda}_{\mathrm{vol}}. \tag{38e}$$

Boundary conditions (BCs) and initial conditions (ICs). For all the designed approaches, we supply the boundary and initial conditions

$$\bar{P}_{\xi}{}^{\Xi}\bar{N}_{\Xi}=0 \qquad \text{for } \Xi=-\tfrac{1}{2}L_{\mathrm{in}},\ \Xi=\tfrac{1}{2}L_{\mathrm{in}},\ \text{and } t\in\,]t_{\mathrm{in}},t_{\mathrm{fin}}], \tag{39a}$$

$$\bar{\omega}=\omega_{\mathrm{env}} \qquad \text{for } \Xi=-\tfrac{1}{2}L_{\mathrm{in}},\ \Xi=\tfrac{1}{2}L_{\mathrm{in}},\ \text{and } t\in\,]t_{\mathrm{in}},t_{\mathrm{fin}}], \tag{39b}$$

$$\bar{\omega}=\omega_{\mathrm{env}} \qquad \text{for } \Xi\in\left]-\tfrac{1}{2}L_{\mathrm{in}},\tfrac{1}{2}L_{\mathrm{in}}\right[\ \text{and } t=t_{\mathrm{in}}, \tag{39c}$$

$$\bar{K}^{R}{}_{R}=\bar{K}^{\Theta}{}_{\Theta}=\bar{K}^{\Xi}{}_{\Xi}=1 \qquad \text{for } \Xi\in\left]-\tfrac{1}{2}L_{\mathrm{in}},\tfrac{1}{2}L_{\mathrm{in}}\right[\ \text{and } t=t_{\mathrm{in}}. \tag{39d}$$

In the Cahn–Hilliard model, together with (39a), (39b) and (39c), we supply the boundary and initial conditions

$$-\mathfrak{M}\left(\frac{\bar{\mu}_{\boldsymbol{K}}}{\bar{J}_{\boldsymbol{K}}}\right)_{,\Xi}\bar{N}_{\Xi}=0 \quad \text{for } \Xi=-\tfrac{1}{2}L_{\mathrm{in}},\ \Xi=\tfrac{1}{2}L_{\mathrm{in}},\ \text{and } t\in\,]t_{\mathrm{in}},t_{\mathrm{fin}}], \tag{40a}$$

$$-\beta\,\bar{J}_{\boldsymbol{K},\Xi}\,\bar{N}_{\Xi}=0 \qquad \text{for } \Xi=-\tfrac{1}{2}L_{\mathrm{in}},\ \Xi=\tfrac{1}{2}L_{\mathrm{in}},\ \text{and } t\in\,]t_{\mathrm{in}},t_{\mathrm{fin}}], \tag{40b}$$

$$\bar{J}_{\boldsymbol{K}\mathrm{in}}(\Xi)=\begin{cases}0.1\tanh\left(-\dfrac{\Xi+L_{\mathrm{in}}/4}{\epsilon L_{\mathrm{in}}}\right)+1.10, & \Xi\in\left[-\tfrac{1}{2}L_{\mathrm{in}},0\right],\\[2ex] 0.1\tanh\left(\dfrac{\Xi-L_{\mathrm{in}}/4}{\epsilon L_{\mathrm{in}}}\right)+1.10, & \Xi\in\left]0,\tfrac{1}{2}L_{\mathrm{in}}\right],\end{cases} \tag{40c}$$

where ϵ is a dimensionless parameter. Finally, to prevent rigid body motions, we set $\bar{u}(0,t)=0$, for all $t\in[t_{\mathrm{in}},t_{\mathrm{fin}}]$, in accordance with the symmetry of the problem. We also mention that (8e) and (12e) are automatically satisfied since $\boldsymbol{K}$ is diagonal for the simulations performed.

6.2. ***Numerical simulations.*** The numerical solution of (35a)–(35e) for the approach A1, and of (38a)–(38e) for the approach A2, together with the BCs and ICs (39a)–(39d), is carried out by means of the commercial software Comsol Multiphysics™ v. 5.3a [COMSOL 2016]. In the following, we do not show the simulations of the mixed approach because, for the considered benchmark problem and material parameters, the condition $\omega\neq\omega_{\mathrm{cr}}$ is always true, so that the mixed approach and the approach A1 coincide.

Figure 1(a) presents the trend of the axial displacement field $\bar{u}$. For all the considered cases, our results are qualitatively coherent with those obtained by [Di Stefano et al. 2018; Grillo et al. 2019b; Licari 2021], in spite of the different scenarios studied in each of these cases. For the approach A1, the magnitude of $\bar{u}$ becomes appreciably higher, as time goes by, than the one computed with the approach A2. This is consistent with the fact that, as visible in Figure 1(b), the axial component of the growth tensor $\bar{K}^{\Xi}{}_{\Xi}$ is greater when it is computed by

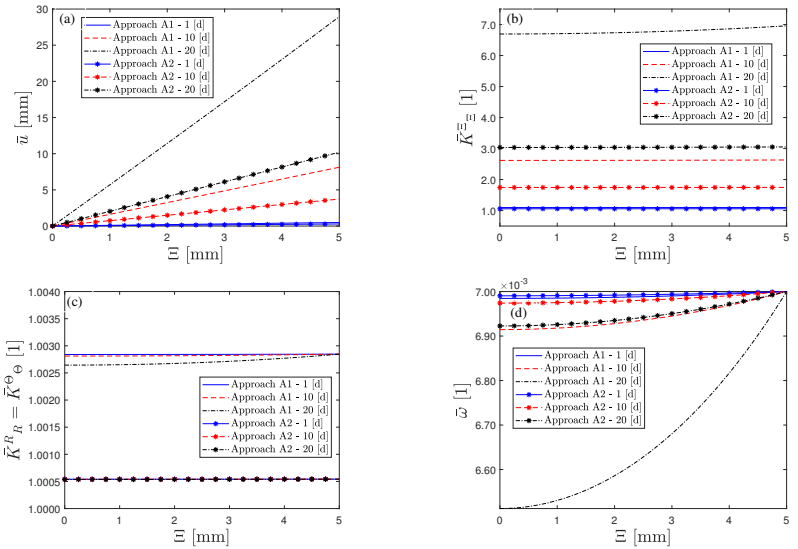

Figure 1. Spatial distribution, at three different times, of $\bar{u}$ (panel (a)), of $\bar{K}^{\Xi}{}_{\Xi}$ and $\bar{K}^{R}{}_{R} = \bar{K}^{\Theta}{}_{\Theta}$ (panels (b) and (c)), and of $\bar{\omega}$ (panel (d)). The considered parameters are given in Table 1.

following the approach A1 rather than A2. This is true also for the radial and the circumferential components of the growth tensor, $\bar{K}^{R}{}_{R}$ and $\bar{K}^{\Theta}{}_{\Theta}$, as reported in Figure 1(c). One fundamental aspect, highlighted by Figures 1(b) and (c), is that $\bar{K}^{\Xi}{}_{\Xi}$ is greater than $\bar{K}^{R}{}_{R} = \bar{K}^{\Theta}{}_{\Theta}$. This implies that the growth tensor $\boldsymbol{K}$ loses the spherical symmetry prescribed by the initial conditions, thereby quite naturally describing a transition towards *anisotropic growth* (in fact, *transversely isotropic* growth) and anisotropic mass distribution within the tissue. We also notice that $\bar{K}^{R}{}_{R} = \bar{K}^{\Theta}{}_{\Theta}$ and $\bar{K}^{\Xi}{}_{\Xi}$ are almost uniformly distributed in the computational domain (see Figure 1(b) and (c)). Such a trend is due to the fact that the effect of $\boldsymbol{Q}$ is rather weak in these simulations, because $\bar{\omega}$ is almost uniform in Ξ, as reported in Figure 1(d). These results are novel with respect to those reported by Licari [2021], who, in lieu of $\boldsymbol{Q}$, used a constant and purely deviatoric tensor that, being independent of the nutrients' mass fraction, did not resolve the direct influence of the nutrients on the differences between the axial and the transversal components of the growth tensor.

In Figure 2, we plot the source of mass $\bar{R}_{\gamma}$, both for A1 and for A2, and we observe significant quantitative discrepancies in the trends of this quantity. This is due to the very nature of the two considered approaches, since, in A1, $\bar{R}_{\gamma} = \bar{R}_{\gamma(\mathrm{ph})}$ is prescribed a priori, while, in A2, $\bar{R}_{\gamma}$ is computed a posteriori, which means that we cannot have control on what it will be. Again, the approach A2 predicts trends that confirm qualitatively and generalize the preliminary results reported by [Licari 2021].

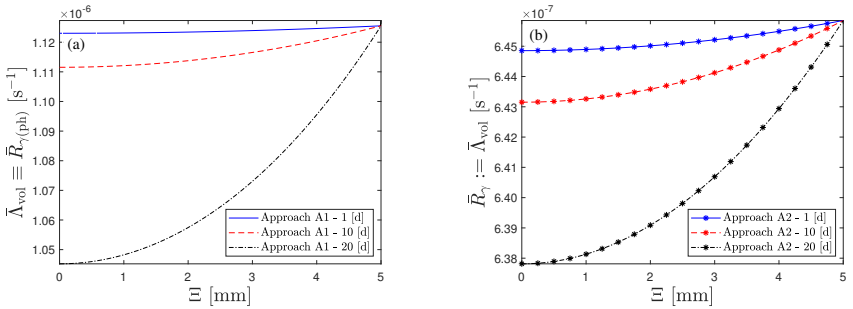

Figure 2. Spatial distribution, at three different times, of $\bar{\Lambda}_{\mathrm{vol}}$, for both the approach A1 (panel (a)) and the approach A2 (panel (b)). The considered parameters are given in Table 1.

In Figure 3, we plot the Lagrange multipliers of the approach A1, obtained once the motion and the growth tensor are computed. We notice that $\bar{\mu}_{\boldsymbol{K}}$ tends to become less uniform for increasing time, and acquires its minimum (maximum of its absolute value) close to the specimen's boundary, which is where $\bar{R}_{\gamma(\mathrm{ph})}$ takes on its highest value. Finally, the trends of $\bar{\mu}_{\mathfrak{T}}$ follow the result $\bar{\mu}_{\mathfrak{T}} = -\bar{\mu}_{\boldsymbol{K}}\bar{R}_{\gamma(\mathrm{ph})}$ and, in particular, have sign opposite to $\bar{\mu}_{\boldsymbol{K}}$ since, in our numerical experiments, $\bar{R}_{\gamma(\mathrm{ph})}$ is always positive. Clearly, since $\bar{\mathcal{Y}}_{\mathrm{u}} - \bar{\mathcal{Z}} = -\bar{\mu}_{\mathfrak{T}}$, the trends of $\bar{\mathcal{Y}}_{\mathrm{u}} - \bar{\mathcal{Z}}$ are specular to those of $\bar{\mu}_{\mathfrak{T}}$. They are nonzero and do not change their sign, since the growth law is always positive. In this respect, $\bar{R}_{\gamma(\mathrm{ph})}$ dictates, in this simulation, the magnitude of this Lagrange multiplier in the approach A1. Indeed, if $\bar{R}_{\gamma(\mathrm{ph})}$ were zero, the constraint $\bar{\Lambda}_{\mathrm{vol}} = \bar{R}_{\gamma(\mathrm{ph})} \equiv 0$ would become time-independent and holonomic, and the force balance $(\bar{\mathcal{Y}}_{\mathrm{u}} - \bar{\mathcal{Z}}) + \bar{\mu}_{\mathfrak{T}} = 0$ would be trivially satisfied, with each summand being null.

We now turn to the solution of the generalized Cahn–Hilliard model presented in Sections 4 and 6.1, for the case of an initial distribution of $\bar{\jmath}_{\boldsymbol{K}}$ that, for symmetry

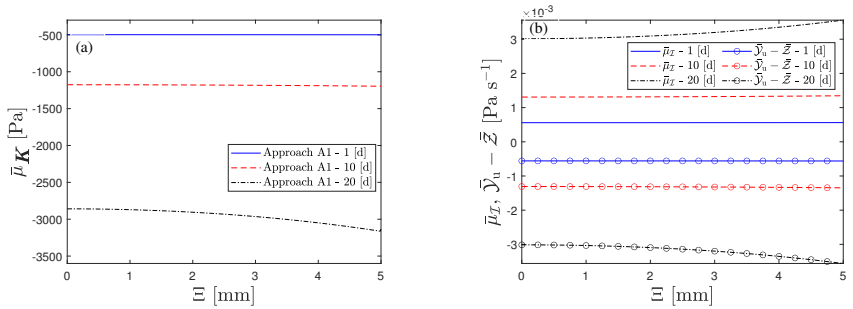

Figure 3. Spatial distribution, at three different times, of $\bar{\mu}_{\boldsymbol{K}}$ (panel (a)) and of $\bar{\mu}_{\mathfrak{T}}$ and $\bar{\mathcal{Y}}_{\mathrm{u}} - \bar{\mathcal{Z}}$ (panel (b)), computed within the approach A1. The considered parameters are given in Table 1.

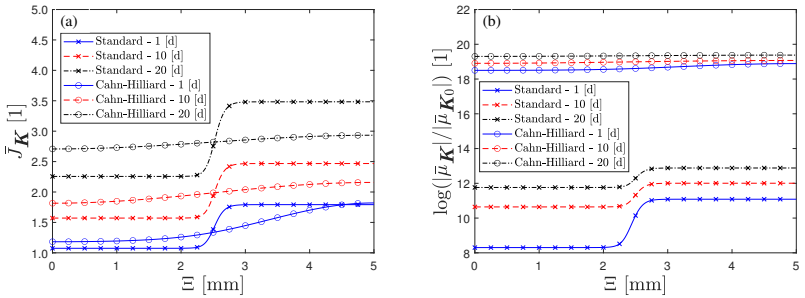

Figure 4. Spatial distribution, at three different times, of $\bar{j}_{\boldsymbol{K}}$ and $\bar{\mu}_{\boldsymbol{K}}$ for the Cahn–Hilliard model, normalized with respect to $\bar{\mu}_{\boldsymbol{K}0} = 1$ Pa. The considered parameters are given in Table 1.

reasons, is given the shape of a kink-antikink. This choice of the initial condition is done to introduce a sufficient (initially localized) inhomogeneity in the model. As shown in Figure 4(a), the diffusion described by the Cahn–Hilliard model spreads the initial inhomogeneity of $\bar{j}_{\boldsymbol{K}}$, and yields curves that, compared to those obtained with the standard model, tend to become constant with increasing time. While the results predicted by the standard model seem to be translated upwards with increasing difference in absolute value between the values of $\bar{j}_{\boldsymbol{K}}$ at $\Xi = 0$ and $\Xi = L_{\text{in}}/2$, this behavior cannot be observed with the Cahn–Hilliard model. Indeed, although the upward translation of the curves is still present, the tendency of the curves to become constant induces a reduction of the absolute value of the difference of the values of $\bar{j}_{\boldsymbol{K}}$ attained at $\Xi = 0$ and $\Xi = L_{\text{in}}/2$. Whereas the global trend of moving the $\bar{j}_{\boldsymbol{K}}$ curves upwards might be a consequence of growth, i.e., of the positive sign of $\bar{R}_{\gamma(\text{ph})}$, the spreading of the initial inhomogeneity is a consequence of the Cahn–Hilliard model. A final remark concerns the Lagrange multiplier $\bar{\mu}_{\boldsymbol{K}}$, which is plotted in semilogarithmic scale and normalized with respect to $\bar{\mu}_{\boldsymbol{K}0}$ in Figure 4(b). Also in this case, the curves of $\log(|\bar{\mu}_{\boldsymbol{K}}|/|\bar{\mu}_{\boldsymbol{K}0}|)$ exhibit a global translation upwards since, for increasing growth, the magnitude of the Lagrange multiplier must increase. Both for the standard and the Cahn–Hilliard model, the curves spread the initial inhomogeneity. However, as expected, the spreading is much more pronounced for the Cahn–Hilliard model, which predicts also higher values of $\log(|\bar{\mu}_{\boldsymbol{K}}|/|\bar{\mu}_{\boldsymbol{K}0}|)$.

7. Conclusions

As predicted in Section 7 of [Grillo and Di Stefano 2023a], and as confirmed by the numerical results presented here, the crucial difference between the approaches A1 and A2 stems from the role of the Eshelby stress tensor. In fact, within the approach A2, the growth of the tumor does not directly descend from the availability

of nutrients, while it is remarkably affected by the Eshelby stress tensor, by the external force $\boldsymbol{Z}$ (which, however, is determined by the nutrients' mass fraction and its gradient), and by their combination. In this respect, $\operatorname{tr}\boldsymbol{H}$ contributes to the determination of R_γ both directly, through $-\operatorname{tr}\boldsymbol{H}$ in (14) (see also [Ambrosi and Guana 2007]), and indirectly, through

$$\hat{\wp}\circ(\boldsymbol{F},\boldsymbol{K}) = -\tfrac{1}{3}\operatorname{tr}\boldsymbol{\sigma} = -J^{-1}\Psi_{\mathrm{R}} + \tfrac{1}{3}J^{-1}\operatorname{tr}\boldsymbol{H}, \tag{41}$$

which features in $\hat{\Gamma}_{\mathrm{a}}\circ(\boldsymbol{F},\boldsymbol{K},\omega)$, as defined in (17c). On the other hand, within the approach A1, the nutrients define the growth law $R_{\gamma(\mathrm{ph})}$, while $\operatorname{tr}\boldsymbol{H}$ is limited to modulate the phenomenological expression of $R_{\gamma(\mathrm{ph})}$ through $\hat{\wp}\circ(\boldsymbol{F},\boldsymbol{K})$. Thus, the leading role is given to the nutrients' mass fraction, which can activate either the accretion of mass or its resorption. Coherently with the explanation given above, the difference in the role played by $\operatorname{tr}\boldsymbol{H}$ in the approaches A1 and A2 appears manifest through significant quantitative discrepancies in the trend of the source and sink of mass. This is due to the way in which the two approaches are conceived, as anticipated in Section 3. Indeed, in the approach A2, the source and sink of mass is computed through the identification $\bar{R}_\gamma := \bar{\Lambda}_{\mathrm{vol}}$, and a posteriori, i.e., once $\bar{K}^{R}{}_{R}$, $\bar{K}^{\Theta}{}_{\Theta}$, and $\bar{K}^{\Xi}{}_{\Xi}$ are determined by solving (38a)–(38e), and $\bar{\Lambda}_{\mathrm{vol}}$ is given by calculating the trace [Ambrosi and Guana 2007; Grillo et al. 2019a]

$$\bar{\Lambda}_{\mathrm{vol}} = \frac{\dot{\bar{K}}^{R}{}_{R}}{\bar{K}^{R}{}_{R}} + \frac{\dot{\bar{K}}^{\Theta}{}_{\Theta}}{\bar{K}^{\Theta}{}_{\Theta}} + \frac{\dot{\bar{K}}^{\Xi}{}_{\Xi}}{\bar{K}^{\Xi}{}_{\Xi}}. \tag{42}$$

Hence, as predicted by (14) and (38b)–(38d), each component of the Eshelby stress tensor contributes to determine the components of the growth tensor and, thus, $\bar{\Lambda}_{\mathrm{vol}}$ (see also [Licari 2021]). In the approach A1, instead, the source and sink of mass is prescribed phenomenologically a priori as $R_\gamma \equiv R_{\gamma(\mathrm{ph})}$, and $\bar{\Lambda}_{\mathrm{vol}}$ is determined accordingly, as prescribed by (35b), which becomes a *constraint* [Grillo et al. 2019b; Grillo and Di Stefano 2023b; 2023c]. Consequently, the role of $\operatorname{tr}\boldsymbol{H}$ is the one that the modeler deems appropriate for $R_{\gamma(\mathrm{ph})}$.

Another fundamental aspect is that $\bar{K}^{\Xi}{}_{\Xi}$ is greater than $\bar{K}^{R}{}_{R} = \bar{K}^{\Theta}{}_{\Theta}$, thereby meaning that the present model is not limited to describe isotropic growth, only. In fact, in our approaches, both the growth-conjugated external force, $\boldsymbol{Z}$, and the Eshelby stress tensor, $\boldsymbol{H}$, supply preferred directions along which $\boldsymbol{K}$ evolves, the medium grows and the mass within it is distributed (see also [Ambrosi and Guana 2007; Licari 2021]).

The last part of this work has been dedicated to the study of the approach A1 formulated in the case of a growth tensor that is *"assumed to be spherical from the outset"* [Grillo and Di Stefano 2023b]. This has been done for two main reasons. First, we wanted to show how such a situation, presented in some pioneering papers on tumor growth (see, e.g., [Ambrosi and Preziosi 2002]), can be recovered by formulating growth as a constrained mechanical problem [Grillo et al. 2019b; Grillo

and Di Stefano 2023b; 2023c]. In particular, we did it when we compared in Figure 4 the results of the Cahn–Hilliard model with those of the "standard" one, obtained for $\mathfrak{M} = 0$, $\beta = 0$, and $\upsilon = 0$. Second, our purpose was to include mass diffusion and to interpret it in light of the results presented by [Gurtin 1996] as the movement of *"defects"*, or *"inhomogeneities"* [Epstein and Maugin 2000; Epstein 2005], relative to the motion of the tumor. In our opinion, Gurtin's formulation of the Cahn–Hilliard model, suitably adapted to our problem as shown by [Grillo and Di Stefano 2023b], offers a rather natural theoretical background for accomplishing this task. On top of that, however, we emphasize that the formulation of growth in terms of Gurtin's view of the Cahn–Hilliard model is, from our perspective, paradigmatic. This is because the hypothesis of spherical growth tensor, which implies $\boldsymbol{K}$ to possess only one degree of freedom (described, in fact, by $J_{\boldsymbol{K}}$), clarifies completely the need for a constrained approach, if the mass source and sink has to be regarded as known from the outset. Indeed, the form of (23a) and (23b) strongly suggests to use the mass balance law (23a), i.e., the constraint, to determine the Lagrange multiplier $\mu_{\boldsymbol{K}}$, and the dynamic equation (23b) for computing $J_{\boldsymbol{K}}$. This way of proceeding, in turn, allows to weigh the "cost" of the imposed constraint through the evaluation of $\mu_{\boldsymbol{K}}$. In passing, we notice that our solution of the Cahn–Hilliard IBVP has been obtained by direct numerical simulations. However, we are aware of publications dedicated to the mathematical analysis connected with problems of this type, including strain gradient elasticity (see, for example, [Eremeyev and dell'Isola 2022]).

Note that the perspective just depicted remains valid also in the limit case of vanishing $\mathfrak{M}$ and β. In this situation, one may still use (23a) for determining $\mu_{\boldsymbol{K}}$ through the Schur complement technique, and (23b) for determining $J_{\boldsymbol{K}}$. However, also another path is possible: one may compute $J_{\boldsymbol{K}}$ directly from (23a), which in many papers is regarded as a mere closure condition (see, for example, [Ambrosi and Mollica 2002; Mascheroni et al. 2016; 2018; Giverso and Preziosi 2019]), so that (23b) seems unnecessary. Still, this is not the case, because the Lagrange multiplier provides an estimate of the reaction to the imposed constraint.

Acknowledgements

The authors thank Prof. Luigi Preziosi for the rationale behind the phenomenological growth law $R_{\gamma(\mathrm{ph})}$, Ms. Francesca Ballatore for possible applications of the growth-conjugated, generalized external force $\boldsymbol{Z}$, Ms. Valentina Licari for discussions about the numerical simulations preliminary to this work, and Mr. Alessandro Giammarini and Mr. Andrea Pastore for very helpful discussions concerning the numerical implementation of the Cahn–Hilliard model. A. Grillo is partially funded by the *Dipartimento di Eccellenza*, Politecnico di Torino (Italy), Project No. E11G18000350001. S. Di Stefano acknowledges *Regione Puglia* in the context

of the REFIN research project *"Riciclo di materiali e sostenibilità*: *modelli di delaminazione per dispositivi laminati"* and INdAM (National Institute of High Mathematics) in the context of *"Progetto Giovani GNFM* 2020-2022*"*. This work is partially supported by MIUR (Italian Ministry of Education, University and Research) through the PRIN project n. 2017KL4EF3 on *"Mathematics of active materials*: *From mechanobiology to smart devices."*

References

[Agosti et al. 2018] A. Agosti, C. Cattaneo, C. Giverso, D. Ambrosi, and P. Ciarletta, "A computational framework for the personalized clinical treatment of glioblastoma multiforme", *ZAMM Z. Angew. Math. Mech.* **98**:12 (2018), 2307–2327.

[Ambrosi and Guana 2007] D. Ambrosi and F. Guana, "Stress-modulated growth", *Math. Mech. Solids* **12**:3 (2007), 319–342.

[Ambrosi and Guillou 2007] D. Ambrosi and A. Guillou, "Growth and dissipation in biological tissues", *Contin. Mech. Thermodyn.* **19** (2007), 245–251.

[Ambrosi and Mollica 2002] D. Ambrosi and F. Mollica, "On the mechanics of a growing tumor", *Internat. J. Engrg. Sci.* **40**:12 (2002), 1297–1316.

[Ambrosi and Preziosi 2002] D. Ambrosi and L. Preziosi, "On the closure of mass balance models for tumor growth", *Math. Models Methods Appl. Sci.* **12**:5 (2002), 737–754.

[Andreucci et al. 2022] D. Andreucci, A. M. Bersani, E. Bersani, F. J. León Trujillo, and S. Marconi, "A 3d mathematical model of coupled stem cell-nutrient dynamics in myocardial regeneration therapy", *J. Theoret. Biol.* **537** (2022), art. id. 111023.

[Ateshian and Weiss 2010] G. Ateshian and J. Weiss, "Anisotropic hydraulic permeability under finite deformation", *J. Biomech. Engng.* **132**:11 (2010), art. id. 111004.

[Bersani et al. 2020] A. M. Bersani, F. dell'Isola, and P. Seppecher, "Lagrange multipliers in infinite dimensional spaces, examples of application", pp. 1425–1432 in *Encyclopedia of continuum mechanics*, edited by H. Altenbach and A. Öchsner, Springer, 2020.

[Byrne and Preziosi 2003] H. Byrne and L. Preziosi, "Modelling solid tumour growth using the theory of mixtures", *Math. Med. Biol.* **20**:4 (2003), 341–366.

[Casciari et al. 1992] J. J. Casciari, S. V. Sotirchos, and R. M. Sutherland, "Variations in tumor cell growth rates and metabolism with oxygen concentration, glucose concentration, and extracellular pH", *J. Cell. Physiol.* **151**:2 (1992), 386–394.

[Chaplain et al. 2006] M. Chaplain, L. Graziano, and L. Preziosi, "Mathematical modelling of the loss of tissue compression responsiveness and its role in solid tumour development", *Math. Med. Biol.* **23**:3 (2006), 197–229.

[Ciancio et al. 2008] V. Ciancio, M. Dolfin, M. Francaviglia, and S. Preston, "Uniform materials and the multiplicative decomposition of the deformation gradient in finite elasto-plasticity", *J. Non-Equilib. Thermodyn.* **33**:3 (2008), 199–234.

[COMSOL 2016] COMSOL, "COMSOL Multiphysics", 2016, https://www.comsol.com/. Version 5.3a.

[Crevacore et al. 2019] E. Crevacore, S. Di Stefano, and A. Grillo, "Coupling among deformation, fluid flow, structural reorganisation and fibre reorientation in fibre-reinforced, transversely isotropic biological tissues", *Int. J. Nonlinear Mech.* **111** (2019), 1–13.

[dell'Isola and Di Cosmo 2018] F. dell'Isola and F. Di Cosmo, "Lagrange multipliers in infinite-dimensional systems, methods of.", pp. 1432–1440 in *Encyclopedia of continuum mechanics*, edited by H. Altenbach and A. Öchsner, Springer, 2018.

[Di Stefano et al. 2018] S. Di Stefano, A. Ramírez-Torres, R. Penta, and A. Grillo, "Self-influenced growth through evolving material inhomogeneities", *Int. J. Nonlinear Mech.* **106** (2018), 174–187.

[Di Stefano et al. 2022] S. Di Stefano, A. Giammarini, C. Giverso, and A. Grillo, "An elasto-plastic biphasic model of the compression of multicellular aggregates: the influence of fluid on stress and deformation", *Z. Angew. Math. Phys.* **73**:2 (2022), 79.

[DiCarlo and Quiligotti 2002] A. DiCarlo and S. Quiligotti, "Growth and balance", *Mech. Res. Comm.* **29**:6 (2002), 449–456.

[Epstein 2005] M. Epstein, "Self-driven continuous dislocations and growth", pp. 129–139 in *Mechanics of material forces*, edited by P. Steinmann and G. A. Maugin, Adv. Mech. Math. **11**, Springer, 2005.

[Epstein and Maugin 2000] M. Epstein and G. Maugin, "Thermomechanics of volumetric growth in uniform bodies", *Int. J. Plasticity* **16**:7–8 (2000), 951–978.

[Eremeyev and dell'Isola 2022] V. A. Eremeyev and F. dell'Isola, "On weak solutions of the boundary value problem within linear dilatational strain gradient elasticity for polyhedral Lipschitz domains", *Math. Mech. Solids* **27**:3 (2022), 433–445.

[Federico 2012] S. Federico, "Covariant formulation of the tensor algebra of non-linear elasticity", *Int. J. Nonlinear Mech.* **47**:2 (2012), 273–284.

[Federico et al. 2016] S. Federico, A. Grillo, and R. Segev, "Material description of fluxes in terms of differential forms", *Contin. Mech. Thermodyn.* **28**:1-2 (2016), 379–390.

[Giorgio et al. 2019] I. Giorgio, F. dell'Isola, U. Andreaus, F. Alzahrani, T. Hayat, and T. Lekszycki, "On mechanically driven biological stimulus for bone remodeling as a diffusive phenomenon", *Biomechanics and Modeling in Mechanobiology* **18**:6 (2019), 1639–1663.

[Giverso and Preziosi 2019] C. Giverso and L. Preziosi, "Influence of the mechanical properties of the necrotic core on the growth and remodelling of tumour spheroids", *Int. J. of Nonlinear Mech.* **108** (2019), 20–32.

[Grillo and Di Stefano 2023a] A. Grillo and S. Di Stefano, "An *a posteriori* approach to the mechanics of volumetric growth", *Math. Mech. Compl. Sys.* **11**:1 (2023), 57–86.

[Grillo and Di Stefano 2023b] A. Grillo and S. Di Stefano, "A formulation of volumetric growth as a mechanical problem subjected to non-holonomic and rheonomic constraint", *Math. Mech. Solids* **28**:10 (2023), 2215–2241.

[Grillo and Di Stefano 2023c] A. Grillo and S. Di Stefano, "Addendum to "A formulation of volumetric growth as a mechanical problem subjected to non-holonomic and rheonomic constraint"", *Math. Mech. Solids* (2023).

[Grillo and Wittum 2010] A. Grillo and G. Wittum, "Growth and mass transfer in multi-constituent biological materials", pp. 355–358 in *ICNAAM* 2010: *international conference of numerical analysis and applied mathematics* 2010 (Rhodes, Greece, 2010), vol. 1281, edited by T. E. Simos, American Institute of Physics Conference Proceedings **1**, 2010.

[Grillo et al. 2012] A. Grillo, S. Federico, and G. Wittum, "Growth, mass transfer, and remodeling in fiber-reinforced, multi-constituent materials", *Int. J. Nonlinear Mech.* **47**:2 (2012), 388–401.

[Grillo et al. 2019a] A. Grillo, S. Di Stefano, and S. Federico, "Growth and remodelling from the perspective of Noether's theorem", *Mech. Res. Commun.* **97** (2019), 89–95.

[Grillo et al. 2019b] A. Grillo, S. Di Stefano, A. Ramírez-Torres, and M. Loverre, "A study of growth and remodeling in isotropic tissues, based on the Anand–Aslan–Chester theory of strain-gradient plasticity", *GAMM-Mitt.* **42**:4 (2019), art. id. e201900015.

[Gurtin 1996] M. E. Gurtin, "Generalized Ginzburg–Landau and Cahn–Hilliard equations based on a microforce balance", *Phys. D* **92**:3-4 (1996), 178–192.

[Holmes and Mow 1990] M. Holmes and V. Mow, "The nonlinear characteristics of soft gels and hydrated connective tissues in ultrafiltration", *J. Biomech.* **23**:11 (1990), 1145–1156.

[Licari 2021] V. Licari, "Considerazioni sulla possibilità di formulare alcune leggi evolutive della crescita volumetrica di aggregati cellulari come equazioni dinamiche di teorie meccaniche dei processi anelastici", Master's thesis, Politecnico di Torino, 2021, https://webthesis.biblio.polito.it/20788/.

[Lubarda and Hoger 2002] V. Lubarda and A. Hoger, "On the mechanics of solids with a growing mass", *J. Mech. Phys. Solids* **39**:18 (2002), 4627–4664.

[Marsden and Hughes 1983] J. E. Marsden and T. J. R. Hughes, *Mathematical foundations of elasticity*, Prentice-Hall, Englewood Cliffs, NJ, 1983.

[Mascheroni et al. 2016] P. Mascheroni, C. Stigliano, M. Carfagna, D. Boso, L. Preziosi, P. Decuzzi, and B. Schrefler, "Predicting the growth of glioblastoma multiforme spheroids using a multiphase porous media model", *Biomech. Model. Mechanobiol.* **15**:5 (2016), 1215–1228.

[Mascheroni et al. 2018] P. Mascheroni, M. Carfagna, A. Grillo, D. P. Boso, and B. A. Schrefler, "An avascular tumor growth model based on porous media mechanics and evolving natural states", *Math. Mech. Solids* **23**:4 (2018), 686–712.

[Nadile 1950] A. Nadile, "Sull'esistenza per i sistemi anolonomi soggetti a vincoli reonomi di un integrale analogo a quello dell'energia", *Boll. Un. Mat. Ital.* (3) **5** (1950), 297–301.

[Ramírez-Torres et al. 2021] A. Ramírez-Torres, S. Di Stefano, and A. Grillo, "Influence of non-local diffusion in avascular tumour growth", *Math. Mech. Solids* **26**:9 (2021), 1264–1293.

Received 9 Nov 2022. Revised 2 Feb 2023. Accepted 4 Mar 2023.

ALFIO GRILLO: alfio.grillo@polito.it
Dipartimento di Scienze Matematiche "G. L. Lagrange", Politecnico di Torino, Torino, Italy

SALVATORE DI STEFANO: salvatore.distefano@poliba.it
Dipartimento di Ingegneria Civile, Ambientale, Edile, del Territorio e di Chimica, Politecnico di Bari, Bari, Italy

MATHEMATICS AND MECHANICS OF COMPLEX SYSTEMS

msp.org/memocs

MEMOCS is a journal of the International Research Center for the Mathematics and Mechanics of Complex Systems at the Università dell'Aquila, Italy.

See inside back cover or msp.org/memocs for submission instructions.

The subscription price for 2023 is US $195/year for the electronic version, and $255/year (+$25, if shipping outside the US) for print and electronic. Subscriptions, requests for back issues and changes of subscriber address should be sent to MSP.

Mathematics and Mechanics of Complex Systems (ISSN 2325-3444 electronic, 2326-7186 printed) at Mathematical Sciences Publishers, 798 Evans Hall #3840, c/o University of California, Berkeley, CA 94720-3840 is published continuously online.

MEMOCS peer review and production are managed by EditFlow® from MSP.

PUBLISHED BY
mathematical sciences publishers
nonprofit scientific publishing
http://msp.org/

Mathematics and Mechanics of Complex Systems
vol. 11 no. 2 2023

MEMOCS is a journal of the International Research Center for the Mathematics and Mechanics of Complex Systems at the Università dell'Aquila, Italy.